Pacific Northwest
NATIONAL LABORATORY

PNNL-38321

CarbStor

Development, Analysis and Modification of Carbon Storing Model Soil Communities

September 2025

Ryan McClure
Marci Garcia
Natalie Sadler
Tesia Lin
Winston Anthony
Kenton Rod
Sankar Krishnamoorthy
Sharon Zhao
Izabel Stohel

U.S. DEPARTMENT of ENERGY

Prepared for the U.S. Department of Energy
under Contract DE-AC05-76RL01830

DISCLAIMER

PACIFIC NORTHWEST NATIONAL LABORATORY
operated by
BATTELLE
for the
UNITED STATES DEPARTMENT OF ENERGY
under Contract DE-AC05-76RL01830

Printed in the United States of America

Available to DOE and DOE contractors from
the Office of Scientific and Technical Information,
P.O. Box 62, Oak Ridge, TN 37831-0062
www.osti.gov
ph: (865) 576-8401
fox: (865) 576-5728
email: reports@osti.gov

Available to the public from the National Technical Information Service
5301 Shawnee Rd., Alexandria, VA 22312
ph: (800) 553-NTIS (6847)
or (703) 605-6000
email: info@ntis.gov
Online ordering: http://www.ntis.gov

PNNL-38321

CarbStor

Development, Analysis and Modification of Carbon Storing Model Soil Communities

September 2025

Ryan McClure
Marci Garcia
Natalie Sadler
Tesia Lin
Winston Anthony
Kenton Rod
Sankar Krishnamoorthy
Sharon Zhao
Izabel Stohel

Prepared for
the U.S. Department of Energy
under Contract DE-AC05-76RL01830

Pacific Northwest National Laboratory
Richland, Washington 99354

Abstract

Soil microbial communities carry out a number of key processes including plant growth promotion, bioremediation and cycling of nutrients. Carbon cycling is among the most important of these nutrients that are metabolized and processed by the soil microbial community. Many of the carbon inputs are converted to alternative organic forms of carbon that can be used by plants or act as biomass for microbial growth. However, inorganic forms of carbon can also be produced by soil microbial communities including calcium carbonate ($CaCO_3$). Production of calcium carbonate is beneficial for the ecosystem in several ways: it can stabilize soils and improve soil health, especially denser soils with high clay content, it can act as a method of bioremediation, it can serve as an alternative carbon source for plants and it can be a way to store carbon in soil in a stable, inorganic manner for the long term. While the chemistry surrounding individual species carrying out this process is well known what is lacking is an understanding of how species interact in a community to drive carbonate production. As all microbial species in soil exist in a community setting gaining this knowledge is critical to our predicting and controlling this microbial phenotype to greatly improve soil health.

The CarbStor project is focused on developing, analyzing and modifying defined microbial soil consortia that express phenotypes at both the species and community level to convert carbon into recalcitrant stable sources such as precipitated carbonate or microbial necromass. To take full advantage of the soil community for this process we will need to fill several key knowledge gaps (**KG**), three of which are the focus of CarbStor. **KG1:** Whether and to what degree microbial communities can be developed that produce precipitated carbon via microbial metabolism. **KG2:** What interspecies interactions drive the individual member phenotypes in defined communities that lead to carbon precipitation. **KG3:** How can these interactions be modified to enhance carbon sequestration beyond what native communities are capable of. *We hypothesize that in a carbon sequestering community only a subset of species will express phenotypes related to carbon storage processes. We also hypothesize that these phenotypes are expressed as a result of interactions with other species in the community that are not involved in carbon storage processes and that these interactions can be harnessed to enhance community carbon sequestration*.

Summary

Our work describes the development and analysis of CSC-A, a microbial consortium derived from soil bacteria, aimed at facilitating calcium carbonate ($CaCO_3$) production through microbial-induced carbonate precipitation (MICP). Community interactions, metabolic processes, and phenotypic diversity were extensively characterized to understand $CaCO_3$ production mechanisms and enhance its potential for carbon sequestration.

Iterative passaging led to standardized consortia dominated by *Bacillus* spp., *Rhodococcus qingshengii*, *Microbacterium*, and *Curtobacterium flaccumfaciens*. Taxonomic analyses revealed evolutionary shifts and stochastic dynamics in community assembly while promoting metabolic complementarity for stable carbonate production. We found that the CSC-A consortium outperformed monocultures of its constituent species as well as the sum produced by each member species, producing 32% more $CaCO_3$, likely due to interspecies metabolic synergy. We also set out to determine what these interspecies interactions might be. Metatranscriptomics highlighted *R. qingshengii* as the metabolic keystone species with critical roles in urea degradation and nitrate metabolism. *B. toyonensis* exhibited niche-expanding roles during the removal of key members. Glutamate also served as a hub molecule for MICP, with glutamine and succinate driving stress adaptation and carbonate precipitation.

As a key link between models and the laboratory work we found that adding succinate in higher amounts during CSC-A growth led to approximately 70% more precipitated $CaCO_3$, showing that our work can help predict and control phenotypes of interest. While *R. qingshengii* is central to urea degradation, *Microbacterium* has high stress tolerance, and *C. flaccumfaciens* specializes in carbohydrate metabolism. These traits collectively enable the consortium's resilience across diverse conditions.

Optimizing urea-rich environments, modifying niche constraints, and engineering interaction networks are key strategies for advancing CSC-A's efficiency in carbonate sequestration. Expanding lab findings to field applications also remains crucial for harnessing its full carbon-storage potential.

Acknowledgments

This research was supported by the Predictive Phenomics Initiative, under the Laboratory Directed Research and Development (LDRD) Program at Pacific Northwest National Laboratory (PNNL). PNNL is a multi-program national laboratory operated for the U.S. Department of Energy (DOE) by Battelle Memorial Institute under Contract No. DE-AC05-76RL01830.Acronyms and Abbreviations

Contents

1.0 Introduction

Much of the focus of soil science is targeted to nutrient cycling, especially cycling of carbon in the soil. To that end, much effort has gone into examining organic forms of carbon in soil (plant roots, microbial biomass, etc), but soil inorganic carbon (SIC) also plays a major role in the soil ecosystem. Inorganic forms of carbon, such as carbonates, can lead to more stable soils, especially those with higher clay content (Chittoori, Burbank, and Islam 2018; Naeimi et al. 2023). Carbonate production has also been shown to be an effective method to bioremediate soils containing heavy metal contamination (S. Wang, Fang, et al. 2023). In addition, soils represent an important carbon sink with the global soil ecosystem able to store up to 2500 gigatons of carbon (Lal 2004). This represents more than 80% of the terrestrial soil carbon, far more than is found in plant biomatter. However, there are significant knowledge gaps that must be filled before we can take real steps to capture inorganic carbon in soil (Okyay et al. 2016). Moving CO_2 from the atmosphere to a soil sink is primarily done through photosynthesis via plant growth and then transferring this carbon belowground as root exudates or plant litter. Plant litter and root exudates are then used as nutrients by soil microbes (Korenblum et al. 2020). In some cases, specific roots exudates are produced by plants to recruit certain microbial species to the root zone (the rhizosphere) to help the plant respond to certain stress conditions such as drought or fungal pathogens (Park, Seo, and Mannaa 2023). Depending on environmental conditions during microbial metabolism of root exudates and other carbon sources, certain fractions of carbon are routed to increased microbial biomass or are respired back into the atmosphere as CO_2. Aside from these routes, other pathways exist for soil carbon, one of which is the production of carbonates (anions) by microbial species (T. Zhu and Dittrich 2016). The carbonate molecules can then combine with cations, such as calcium, in the soil, to produce calcium carbonate, $CaCO_3$, among other molecular species (Phillips et al. 2013). $CaCO_3$ (calcite) is one of the most abundant forms of carbon in the soil, especially arid or semi-arid regions, while other carbonate species, such as dolomite, are more common in sediments (Sparks, Singh, and Siebecker 2022). Once in this form, carbon is much less labile and soluble, making it harder to use as inputs for further microbial metabolism, though it can be released via acidification as a result of human activity (Zamanian, Zhou, and Kuzyakov 2021). This stability means that such carbon can remain in the soil and provide benefits (prolonged stable sequestration, soil stability, etc) for the long term.

One of the most energy efficient and common ways in which microbially induced calcium carbonate precipitation (MICP) is carried out is through urea hydrolysis, or ureolysis, via urease enzymes (Dhami, Reddy, and Mukherjee 2013; Fu, Saracho, and Haigh 2023). Microbial ureolysis produces ammonia and CO_3^{-2}; the former increases the local pH which in turn creates conditions that allow the latter to bind to available cations, such as Ca^{2+}, to form insoluble $CaCO_3$ precipitates (Stocks-Fischer, Galinat, and Bang 1999). A number of soil microbes have been found that can carry out this process including, but not limited to, *Sporosarcina pasteurii* (P. Liu, Zhang, et al. 2021), *Pseudomonas* sp. (feng Su et al. 2019), *Variovorax* sp. (Fujita et al. 2000), *Micrococcus luteus* (X. Liu, Zarfel, et al. 2021) and *Bacillus cereus* (Xuejiao Zhu et al. 2016). An additional way in which production of $CaCO_3$ can be driven by microbes is through expression of carbonic anhydrase enzymes (Occhipinti and Boron 2019). Identified carbonic anhydrase producing soil microbes include *Virgibacillus* (Abdelsamad et al. 2022), *Ralstonia* (Supuran and Capasso 2017)*, and Pseudomonas* (Giri and Pant 2019)*. Carbonic anhydrases may be of even greater interest as their activity* consumes CO_2, rather than urea, to generate carbonate, further reducing total CO_2 levels.

Many of the specific species, as well as the molecular processes and enzymes, that are involved in MICP are well known (Dhami, Reddy, and Mukherjee 2013). However, within the native soil ecosystem no species exists in isolation. The production of $CaCO_3$ by the soil microbiome is an outcome of the complete soil microbial community, not only individual species

but also the interactions they have with other members. These species may include those that do not produce $CaCO_3$ themselves but who may have critical roles at the community level that enhance the production of $CaCO_3$ in the soil as a whole. Many additional processes carried out by the soil microbial community have been found to be driven by the interaction network of these microbial species (e.g. nutrient decomposition or nitrogen fixation) (Gorter, Manhart, and Ackermann 2020; Saraiva et al. 2021). The same is likely true for communities that mineralize carbon. Because $CaCO_3$ production is likely as much a community process as it is a process driven by individual species it is critical for us to understand these community processes if we want to harness the soil microbiome to drive the formation of inorganic forms of carbon.

Despite the need to understand interactions within soil microbiomes related to MICP this is often a difficult goal to reach. The soil microbial community is incredibly complex and direct analysis of this ecological system to fill knowledge gaps is difficult. Recently, success has been seen in reducing the complexity of the soil microbiome into model, representative communities that contain fewer species and are more amenable to -omics assays and other studies designed to better understand the molecular basis of interactions and how they lead to expressed functions (Lozano et al. 2019; Ryan McClure et al. 2022; R. McClure et al. 2020). While caution should be applied to any discoveries made from analysis of a consortium with regard to their relevance to natural, more complex, systems the development and study of such consortia can lead to new, testable hypotheses and fundamental paradigms that can then be tested in the complete and natural system. To that end, the development of a defined, reduced complexity, soil-derived microbial consortium that can carry out MICP would be a major step forward in harnessing soil systems for carbon storage. Here, we describe the development and analysis of a carbon storing consortium (**CSC**) comprised of soil bacteria and show that such a consortium can drive the formation of large amounts of $CaCO_3$ as a result of synergistic interactions between members.

From CSC-A, we also aimed to characterize the metabolic potential of each microbial member, identify their respective functional niche in a complex MICP system, and map potential molecular interactions that may be key to MICP processes. Through the integration of multiple ‘omics methods, we find evidence that the 4-member community encodes diverse functional potential in their genomes, and expression data confirms removing individual species has markedly different effects on the meta-transcriptome. Integrating transcriptomic and metabolomic enrichment during consortia growth in urea identified unique methods utilized by community members for mitigating stress and metabolizing degradation products induced by MICP. Key nitrogen regulators were identified that improve yields in some CSC-A members to reduce utilization of non-optimal amino acid degradation as a nitrogen source. Finally, a set of cross-pathway metabolic reactions, centered around glutamate and succinate as keystone metabolites, drive a community-wide response linked to amino acid metabolism during MICP. This response ultimately allows CSC-A to degrade urea more efficiently than just a single species, resulting in a previously observed phenotype of enhanced calcium carbonate production in the consortium. Our cross-sectional exploration culminated in the identification of species-specific roles in urea-degradation and stress-tolerance, which are important for enhancing MICP processes, laying a foundation for manipulation of metabolic exchanges in future studies to enhance and harness the capabilities of this and other naturally derived carbon sequestering communities.

2.0 Results

Identifying a medium promoting calcium carbonate formation.
Our ultimate goal was the development of a consortium of soil bacteria that is enriched for a $CaCO_3$ formation phenotype. The choice of medium used to evolve this consortium will have a large effect on which species are retained, and which are competed out. To identify which media source might be best for our desired goals, we tested five different media types against three species of bacteria known for their potential to drive $CaCO_3$ production: *S. pasteurii*, *E. coli* MJK2, and *B. subtilis.* All three species grown in B4U and B4UNZ medium induced large amounts of $CaCO_3$ formation. B4U medium led to $CaCO_3$ levels that were between 2.7-fold and 34-fold higher than $CaCO_3$ amounts with either NBU, NBUNZ, or NZECM levels in either *E. coli* or *B. subtilis*. B4UNZ medium led to $CaCO_3$ levels that were between 3.5-fold and 26-fold higher than $CaCO_3$ amounts with either NBU, NBUNZ, or NZECM levels in either *E. coli* or *B. subtilis*. NZECM did lead to very high levels of $CaCO_3$ in *S. pasteurii*. However, the goal of this project was to enrich a diverse set of MICP bacteria, and since NZECM seemed to lead to $CaCO_3$ formation only in one species out of the three tested, its effects might not be applicable to a wide variety of bacterial species, and it was set aside. With these results, we chose to move forward with consortia development using B4U and B4UNZ media. Since media containing urea will tend to enrich for a community containing ureolysis as a pathway to drive carbonate production, we also wanted to explore the effect of other media types. We therefore also chose to develop consortia on the B4U and B4UNZ media lacking urea (B4, B4NZ).

Enriched communities of $CaCO_3$ producing species
We chose to use both agar plate assays and liquid growth assays to evolve our communities (**Figure 1**). While this approach obviously selects only for lab culturable species and would tend to select for fast growing species, this was part of our design. We will need a final consortium of culturable species if we wish to better understand the details of species interactions that drive $CaCO_3$ formation. A faster growing consortium also lends itself better to laboratory work. We also included a phenol red indicator in subsequent platings after an initial week of growth to track changes in pH as carbonate precipitation increases, as the environment becomes more alkaline. Our initial week of growth after agar plating showed a wide variety of isolate colonies; of all media types, B4U medium showed the fewest number of colonies (**Figure 2A**). Growth in liquid media was robust, and several replicate communities showed shifts to a red color (indicating higher pH) (**Figure 2B**). Passaging of plates and liquid growth continued every 3-4 days. In general, communities grown in liquid culture increased the media pH over time (comparing 12-hour timepoints to 72-hour timepoints, data not shown). Notably, there did not seem to be a strong correlation between replicates tubes of the same media type when looking at either increases in pH or white precipitate (hypothesized and later confirmed to be $CaCO_3$) suggesting a large amount of stochasticity in the evolution and expressed phenotypes of replicate communities, this was later supported by 16S rRNA analysis showing that in many cases communities started with similar taxonomic profiles and then diverged with time. In addition to differences in the taxonomic makeup, the small number of replicates here (3) could also be a factor in determining whether certain consortia influence precipitation and pH changes, as could the growth rates of the emerging communities. Communities that are slower growing will lead to less precipitate and pH increases, even if they have the genomic and phenotypic potential to drive $CaCO_3$ production. Using B4 medium, we initially saw a consistent increase in pH in Replicate C, but after week 5 this ceased and subsequent replicate communities with this medium type did not show pH changes or white precipitate. For communities made using B4NZ medium after week 2, Replicate C showed consistent changes in pH; however, white precipitate was not visible in this consortium.

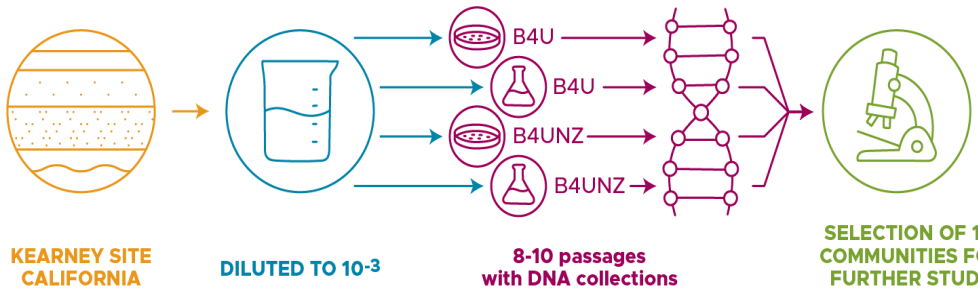

Fig. 1. Schematic of experimental approach. Soil was collected from a field site in California and shipped to Washington state. Soil was diluted and plated on agar plates or used to inoculate liquid media. Every 3-4 days emerging microbial growth was passaged. After 8-10 passages, 1-2 communities were selected for further analysis.

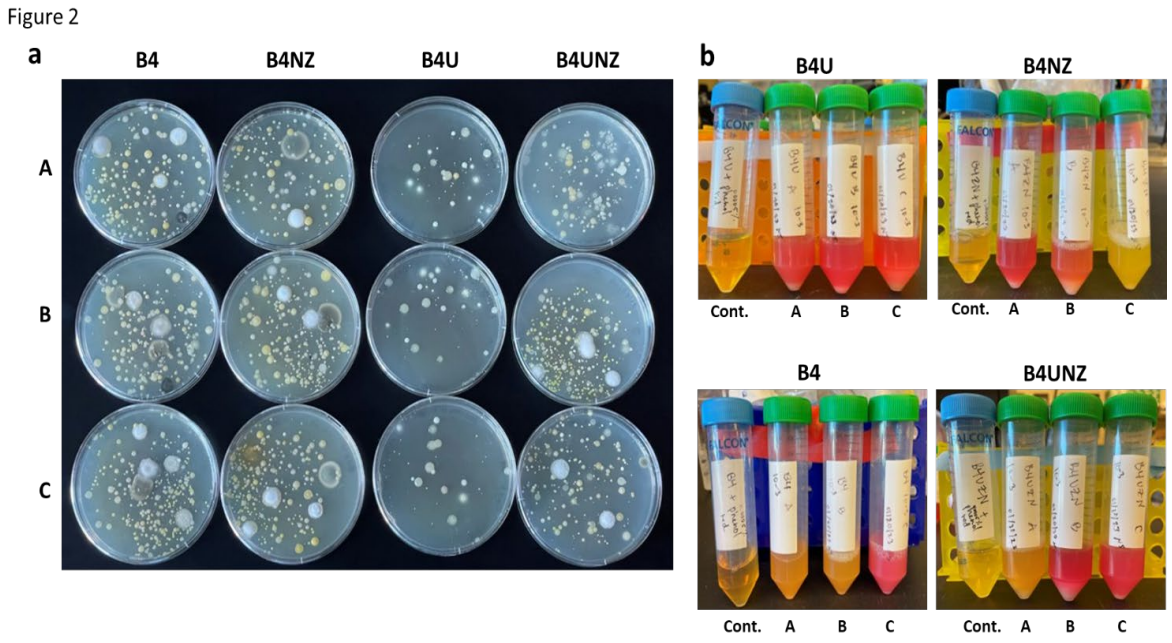

Fig. 2. Early stages of community development. A. Photos of R2A agar plates after one week of growth following spreading of diluted soil. Letters on the vertical indicate replicates. Labels on the horizontal indicate media types (Supplemental Table 1). B. Photos of liquid media after one week of growth following inoculation of soil dilution. Media types are indicated on the top of each picture and inoculated replicates on the bottom. "Cont." indicates the uninoculated control.

For consortia developed using B4U medium, we saw consistent pH changes in Replicate B as well as large amounts of white precipitate. Finally, use of B4UNZ medium showed some variability between replicates, but by the last few weeks, consistent pH changes were noted in Replicates A and B with white precipitate also being observed in both tubes (though less than that with B4U medium) (**Figure 3B**). Looking at consortia developed on plates, we did see more consistent responses across medium types, but still some variability between replicates. Generally, all three replicates from B4NZ medium show consistent increases in pH (color change on plates from yellow to red). A similar trend was also seen with Replicates B and C using B4UNZ medium though this did have some variability (**Figure 3A**). In some cases, white crystals could be seen on the surface of the microbial lawn, but this was more difficult to quantify and verify compared to white precipitate seen in liquid medium.

Selection of Species for a Carbon Storing Consortium

At the conclusion of consortia development, we selected four consortia that appeared to drive the production of the largest amounts of $CaCO_3$ based on visual examination of tubes and plates. These were: plate consortium B4ZN-A, plate consortium B4ZN-C, plate consortium B4UZN-C, and liquid consortium B4UZN-B. Each of these consortia were then diluted to between 10^{-1} and 10^{-3} using R2A medium and plated on R2A agar plates to isolate individual colonies and eventually constituent species. Constituent selection took place after the development of consortia so that we would be more likely to select isolates that would combine to form a stable community. After one week, individual colonies began to emerge. These were collected and replated onto B4UNZ agar plates with phenol red. As we wanted to develop a consortium comprised of species that may drive the production of $CaCO_3$ and those that may not (to understand interactions between species with different phenotypes better) we selected colonies that led to colorimetric changes in the agar plates (indicating increases in pH due to added phenol red) and those that did not (**Figure 4A**), this fulfilled our goal of a consortium that would likely contain $CaCO_3$ forming members as well as members not driving the formation of $CaCO_3$ We also selected those that led to crystals forming on the tops of the colonies (**Figure 4B**) (likely $CaCO_3$ crystals). The variability in color changes on the plates as a function of CFUs was our first indication that not all of the species being isolated from these consortia have a $CaCO_3$ production phenotype. Selected isolates were then passaged at least three more times on R2A agar before being collected for DNA extraction and 16S rRNA Sanger sequencing. We eventually chose 51 isolates to send out for sequencing. In some cases, 16S rRNA Sanger sequencing was repeated twice to ensure correct identification.

16S rRNA sequencing consistently determined many of the same genera and, in some cases, species. This observation was also supported by our 16S rRNA amplicon analysis of all consortia (liquid, plate, medium type, and replicate, **Figure 4C**). Amplicon analysis showed that many of the same species emerge as consortia evolve, but there are some taxonomic differences between consortia and major differences in the abundance of species common to more than one

Figure 3

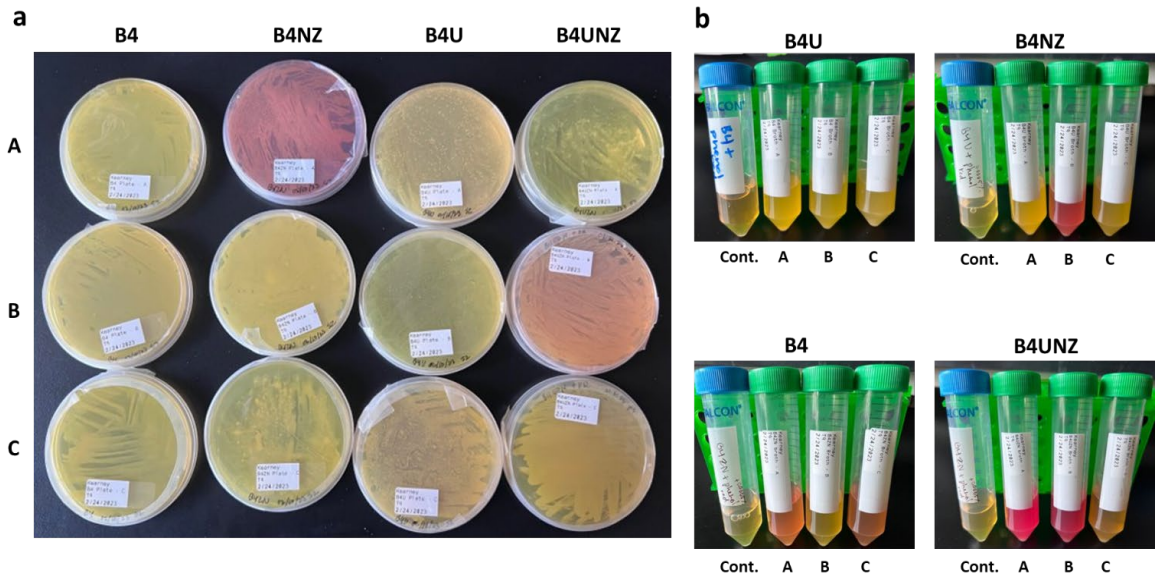

Fig. 3. Final stages of community development. A. Photos of R2A agar plates after nine passages. Letters on the vertical indicate replicates. Labels on the horizontal indicate media types (Supplemental Table 1). B. Photos of liquid media after nine passages. Media types are indicated on the top of each picture and inoculated replicates on the bottom. “Cont.” indicates the uninoculated control.

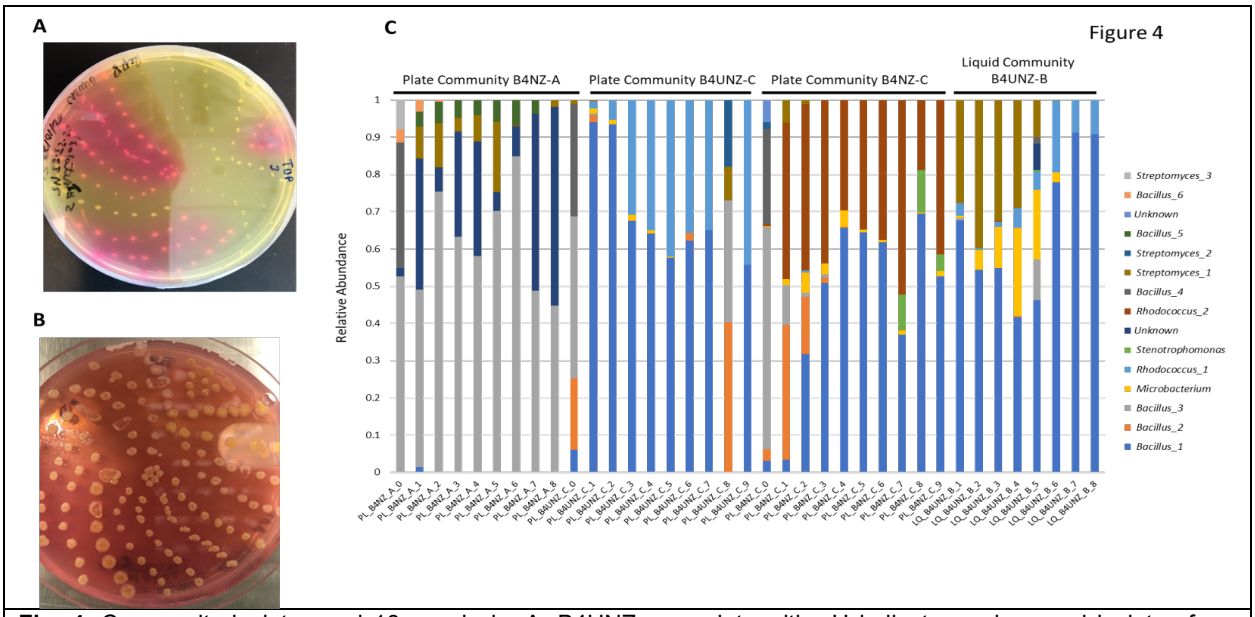

Fig. 4. Community isolates and 16s analysis. A. B4UNZ agar plate with pH indicator and several isolates from evolved communities. Areas of the plate that are pink indicate a local rise in pH. B. The same plate as in (A), but after several more days of growth. Crystalized CaCO3 is visible on the tops of several colonies. C. 16S rRNA amplicon data. Relative abundances are shown on the y-axis. Communities are indicated along the x-axis, and community groups are indicated above. Taxonomies are indicated by color. "Bacillus_3" and "Bacillus_4," for example, indicate Bacillus genera that could be differentiated by 16s but for which the species identity is not known.

consortium depending on the medium type, environment (liquid or plate), and even the replicate. Plate consortium B4ZN-A was comprised almost exclusively of several *Bacilli* species with some *Streptomyces* membership as well. In contrast, plate consortium B4ZN-C was comprised of separate *Bacilli* species as well as very high levels of *Rhodococcus* species and a small amount of *Stenotrophomonas*. The amplicon analysis also showed the importance of sufficient passaging to allow for the greatest amount of consortium stability. With each passage, the consortia generally changed less compared to the previous passage, showing that sufficient passaging can lead to a more stable community. Even in the last few passages, however, some consortia were still changing, though more slowly than at the beginning of the evolution. 16S analysis also provided a closer view on how stochasticity may be a factor in consortium development. PCA plots showed how some environments (plate or liquid) and medium combinations contained consortia that were very similar taxonomically at the start CSC-A development but then diverged. For example, consortia developed in liquid medium with either B4 or B4NZ medium replicate starting consortia and early passages (Week 0 and Week 1) were similar, but as passaging continued (Weeks 4-8), replicate consortia became taxonomically more and more divergent showing that even consortia that start off very similar can rapidly diverge even under the same cultivation conditions. This was also the case with replicate consortia in B4 and B4NZ medium developed on agar plates. However, for consortia developed using B4U or B4UNZ medium (in either liquid medium or on plates), starting consortia were much more diverse, suggesting that initial dilutions of the soil may have led to differences in the start point rather than stochasticity as the consortium developed.

The five taxa that were most commonly found during our isolation of species were *Bacillus thuringiensis*, *Bacillus toyonensis*, *Curtobacterium flaccumfaciens*, *Rhodococcus qingshengii*, and a *Microbacterium* sp. In the case of the two *Bacillus* sp., the *Rhodococcus*, and the *Microbacterium,* the species were often found in the same consortium. The *Curtobacterium* species was only isolated from a single consortium, one grown on agar plates using B4ZN-A medium. Based on the variability in the pH and carbonate producing effect of the five most

common species, as well as their consistent co-emergence from a complex soil community, we chose to include all five species in our test consortium examining $CaCO_3$ production. For *Bacillus thuringiensis*, *Bacillus toyonensis*, *Rhodococcus qingshengii,* and the *Microbacterium* sp. these members were isolated from the same developed consortium. The *Curtobacterium* member was isolated from PI-B4ZN-A. All of these are known soil species, not commonly found in humans. We term this combined test consortium Carbon Storing Consortium A (**CSC-A**).

Growth and pH shifts of member species of CSC-A

We next tested the growth of each of the five member strains of CSC-A on B4UNZ medium. Growth rates of each species can be used as input to begin to hypothesize interactions, and faster growing species that also drive $CaCO_3$ production will be a larger factor in CSC-A carbonate production rates. *Microbacterium* showed initial fast growth and had the highest final O.D. The two *Bacillus* strains (*B. toyonensis* and *B. thuringiensis*) showed similar growth profiles over time though *B. toyonensis* did have a higher O.D.. *Curtobacterium* rapidly increased to a final O.D. of ~1.2 where it remained with a long, stable stationary phase. *Rhodococcus* showed the slowest growth increase but peaked briefly at the highest O.D. Data from *Rhodococcus* was also quite noisy, suggesting significant cell clumping (**Figure 5A**). We also measured the role each species has in changing pH as higher pH levels would lead to a more amenable environment for formation of $CaCO_3$. In most cases, pH changes by individual species were very different than O.D. changes. B4UNZ medium cultured with *Rhodococcus* showed a rapid increase in pH, reaching ~9.0. *Microbacterium* also showed a rapid increase, but the final pH was only slightly above 7.0. Both *Bacillus* strains showed a slower increase in pH ending between *Rhodococcus* and *Microbacterium* (pH of ~7.75). *Curtobacterium* showed the slowest change; pH levels did not begin to rise until roughly 72 hours after the start of the experiment but by 144 hours the pH change was rapidly increasing and had reached greater than 7.5 (**Figure 5B**).

$CaCO_3$ production by each member species of CSC-A and the full consortium

We next grew each member species as well as the combined CSC-A using B4UNZ medium and measured the amount of $CaCO_3$ that precipitated with each strain and in CSC-A. We first took additional steps to confirm that the white precipitate we were seeing in later stages of consortium development was in fact, $CaCO_3$. We used microscopy to confirm that the precipitate exhibits UV excitable autofluorescence, a known characteristic of some polyforms of $CaCO_3$ precipitates. (Yoshida, Higashimura, and Saeki 2010; Zambare et al. 2020). In addition, white precipitate only appears when the pH becomes more basic, allowing for the carbonate to fall out of solution. We confirmed that this precipitate goes back into solution when the pH is lowered by adding acid to the sample. Finally, X-ray diffraction analysis confirmed that 75% of the sample is vaterite, 5% is calcite, and the remaining 20% is amorphous.

We cultured each of the strains independently as well as the complete consortium together and collected $CaCO_3$ samples at 72 hours and 144 hours after the start of the experiment (**Figure 6A**). At 72 hours after the start of the experiment CSC-A was driving the production of large amounts of $CaCO_3$, ~230 mg/L of medium. Among the five strains, only *Rhodococcus* was driving the production of a similar amount of $CaCO_3$, ~280 mg/L, the remaining four members were led to the precipitation of almost no $CaCO_3$, and there was none in a non-inoculated control tube as well. By 144 hours, things were very much the same except higher amounts of $CaCO_3$ were found with *Rhodococcus* (~375 mg/L) and CSC-A (~490 mg/L). At this point, we also noted that CSC-A was producing significantly more $CaCO_3$ than *Rhodococcus* alone. At the 144-hour timepoint we took a closer look at any $CaCO_3$ produced by other members of the community aside from *Rhodococcus* (**Figure 6B**). Again, only small amounts precipitated, but the amounts were higher than the blank uninoculated control with *Curtobacterium* driving the production of the highest amount among the four followed by *Microbacterium* and the two *Bacilli* strains. For each of the three replicate experiments, the sum of the total $CaCO_3$ produced by all member species grown

in monoculture was 366.27, 348.39, and 398.38 mg, while the amount produced by the CSC-A community as a whole was 466.28, 543.45, and 467.16 mg, an average increase of 32% (p-value of 0.014). The fact that CSC-A produces more $CaCO_3$ than the sum of the individual member species at the later timepoint strongly suggest that it is interspecies interactions, not just contributions of species considered in isolation, that lead to the carbon sequestering phenotype of CSC-A.

We next wanted to investigate the taxonomic makeup and stability of CSC-A. We wanted to determine if this consortium was relatively even or was primarily composed of *Rhodococcus*, the only species that drove $CaCO_3$ production in monoculture. We found that when all members were combined, the results led to a fairly even consortium, except for *Microbacterium*, which started at a much lower level. After 72 hours of incubation, the relative species abundance levels of CSC-A were very much the same, suggesting a stable consortium where one member does not overtake the other four, though this may change at 144 hours, beyond the time frame of our 16S rRNA work. There were increases in the amount of *Rhodococcus* and corresponding decreases in *Bacillus thuringiensis* and *Curtobacterium,* but these differences were slight. Thus, the increased $CaCO_3$ we see with the CSC-A community is likely not a result of simply higher relative amounts of *Rhodococcus* but rather something more complex. It is possible that in CSC-A there may be a greater number of *Rhodococcus* cells overall compared to a *Rhodococcus* monoculture but if this were the case it still suggests factors driving faster growth of the community compared to the monoculture and a similar knowledge gap to be filled surrounding interactions.

We also confirmed that CSC-A can produce $CaCO_3$ even when back in native soil over a period of several weeks. We also show that this carbonate production is somewhat resistant to moisture loss (**Figure 7**).

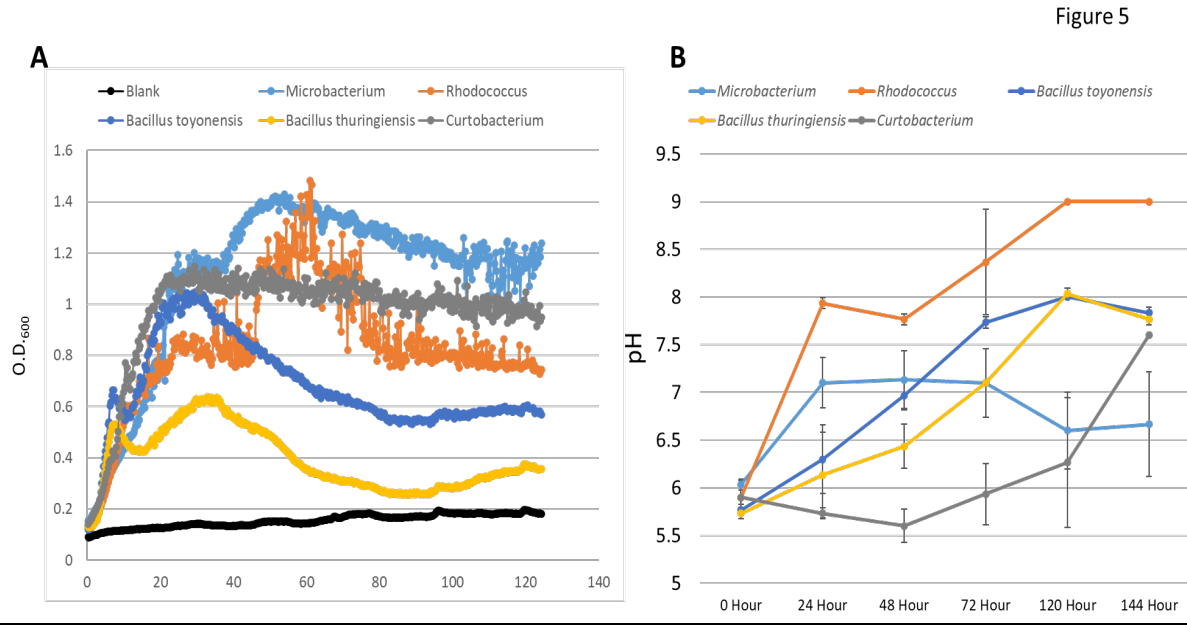

Fig. 5. Growth and pH shifts of CSC-A members. A. Growth curves of CSC-A members (indicated by color). Optical density at 600 nm is on the y-axis and hours are on the x-axis. Error bars indicate standard deviation. B. pH shifts of medium during cultivation of CSC-A members. pH is on the y-axis and hours are on the x-axis. Error bars indicate standard deviation.

Figure 6

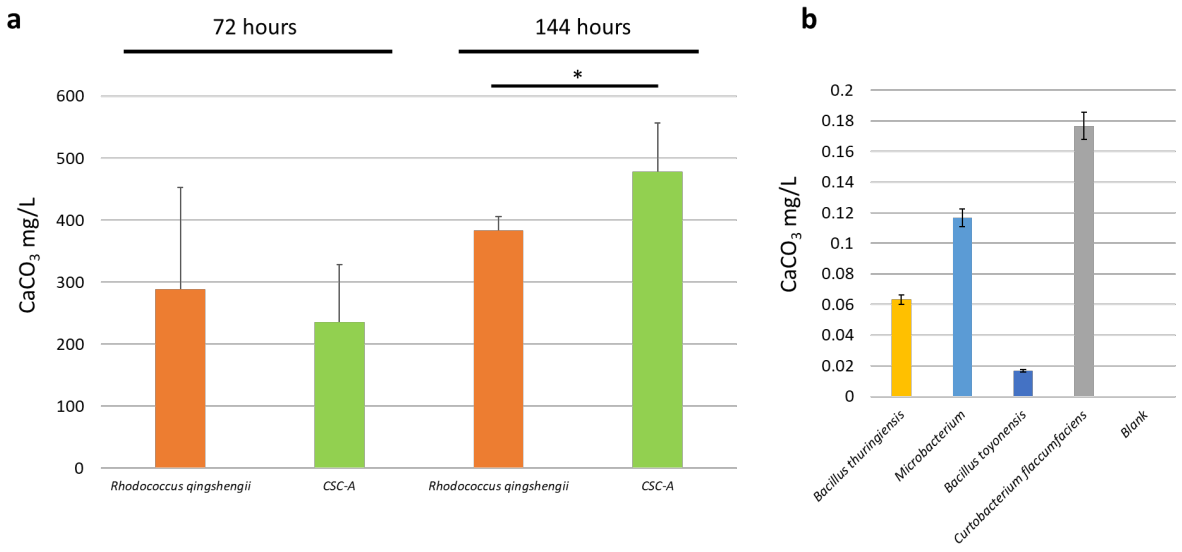

Fig. 6. CaCO3 amounts produced by CSC-A constituents and the community as a whole. A. The amount of CaCO3 is shown in the y-axis. *R. qingshengii* (a major carbonate producer) and the CSC-A community are shown on the x-axis. Two timepoints were analyzed, indicated on the top of the figure. A * indicates a p-value of less than 0.05. B. A zoomed in view of some of the constituents of CSC-A that produce small amounts of CaCO3 at the 144-hour timepoint.

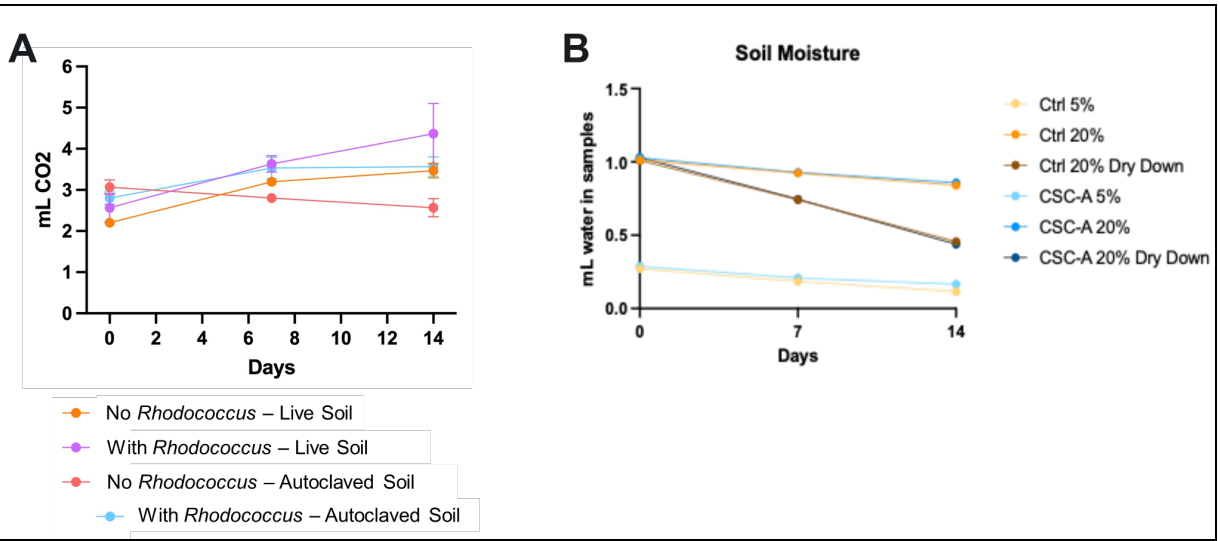

Fig. 7. Production of $CaCO_3$ by CSC-A or CSC-A members in soil. **A)** Production of $CaCO_3$ in live or autoclaved soil by *R. qingshengii*. The y-axis (mL of CO_2) refers to the amount of CO_2 produced after exposing soil to acid to dissolve the $CaCO_3$. The amount of CO_2 produced is directly related to the amount of $CaCO_3$ in the soil. **B)** Production of $CaCO_3$ by CSC-A in soil as moisture is lessened.

CSC-A is a genetically diverse soil microbial consortium with each member encoding unique stress tolerance traits and niche adaptations

The CSC-A consortium was previously isolated from agricultural soil sourced from the state of California. The community is made of four members, which were isolated, cultured, and sequenced. Reads were de novo assembled to identify their taxonomic assignment and estimate their functional and metabolic potential. Development of this community is detailed in a previous publication. Three of the four community members were identified to species level assignment: *Rhodococcus qingshengii* and *Curtobacterium flaccumfaciens* from the Actinomycetota phylum and *Bacillus toyonensis* from the Bacillota phylum. One member was classified to the genus *Microbacterium* within the phylum Actinomycetota; however, this isolate fell outside the 95% average nucleotide identity threshold for assignment to any of the type strains within the genus.

R. qingshengii exhibited the largest genome at 7.2 Mb, followed by *B. toyensis* at 5.3 Mb. The *Microbacterium sp.* (hereafter referred to as *Microbacterium*) and *C. flaccumfaciens* both had smaller genomes at 3.9 and 3.8 Mb, respectively. *C. flaccumfaciens* was estimated to have the longest minimum generation time (MGT), (2.1 h^{-1}) as well as the highest optimum growth temperature (OGT) and GC content at 34.1°C and 71%, respectively. In order of decreasing MGT, *Microbacterium*, *R. qingshengii*, and *B. toyonensis* had estimated MGTs of 1.2, 1.2, and 0.4 (h^{-1}), respectively. The community also exhibited a wide OGT range, with *B. toyensis*, *Microbacterium*, and *R. qingshengii* estimated to grow best at 31.9°C, 31.8°C, and 24.3°C (temperatures routine to the California site where these species were isolated form), respectively. Thus, CSC-A contains a diverse set of species with a range of genetic characteristics and growth dynamics.

To further characterize the functional potential of the community, we mapped the protein sequences from each member to a unique profile of functional trait representations (**Figure 8**). *R. qingshengii* is the only consortia member with a genome containing urea transport and a urease system, supporting our prior work showing that this species produces large amounts of $CaCO_3$. *Microbacterium* had some of the highest trait representation for resource scavenging, such as the transport of aromatic compounds, various polysaccharides, as well as small molecules such as metal ions, sulfur, and siderophores. While *Microbacterium* primarily exhibited stress response traits assigned to two-component systems*, B. toyensis* instead carried a relatively large genetic complement of stress mitigation (general, heat, cold, and pH) through ATP−dependent proteases. *C. flaccumfaciens* exhibited the unique ability to transport and depolymerization multiple complex carbohydrates: xylan, heteromannan, cellulose, and mixed-linkage glucans. *C. flaccumfaciens* also possesses genes increasing tolerance to osmotic and generalized stress through bacterial exopolysaccharide (EPS) biosynthesis as well as biofilm formation. Finally, *C. flaccumfaciens* and *Microbacterium* both shared a set of traits related to saccharide transport, stress tolerance via heat-shock proteins, and the ability to degrade chitin. Given the varied functional potential, we anticipated a large degree of specialization during co-culture, and that removing individual members would significantly perturb community metabolic output.

R. qingshengii loss results in a larger perturbation to the metatranscriptome compared to C. flaccumfaciens

Given the unique metabolic potential found in each member of CSC-A, we sought to quantify the impact removing specific community members would have on the metatranscriptome during growth with urea. An initial metabolic exchange model generated using draft genome scale models mapped the unique potentials of each species; it ultimately suggested that at most exchange interactions were centered around *C. flaccumfaciens.* The exchange model predicts it to serve as a receiver for metabolites from all three other consortia members, simultaneously acting as a metabolite donor for *R. qingshengii*. With this preliminary information, we selected two community perturbations for expression profiling in two separate experiments: removal of *C. flaccumfaciens* or *R. qingshengii*. We selected *C. flaccumfaciens* as it was estimated to have the longest MGT and highest OPT, and we expected it to be central to metabolic exchange in our consortia. *R. qingshengii* is the only member with a detected urea degradation system and prior

analysis indicates *R. qingshengii* produced the highest amount of $CaCO_3$, thus we were eager to see how CSC-A would respond to its removal.

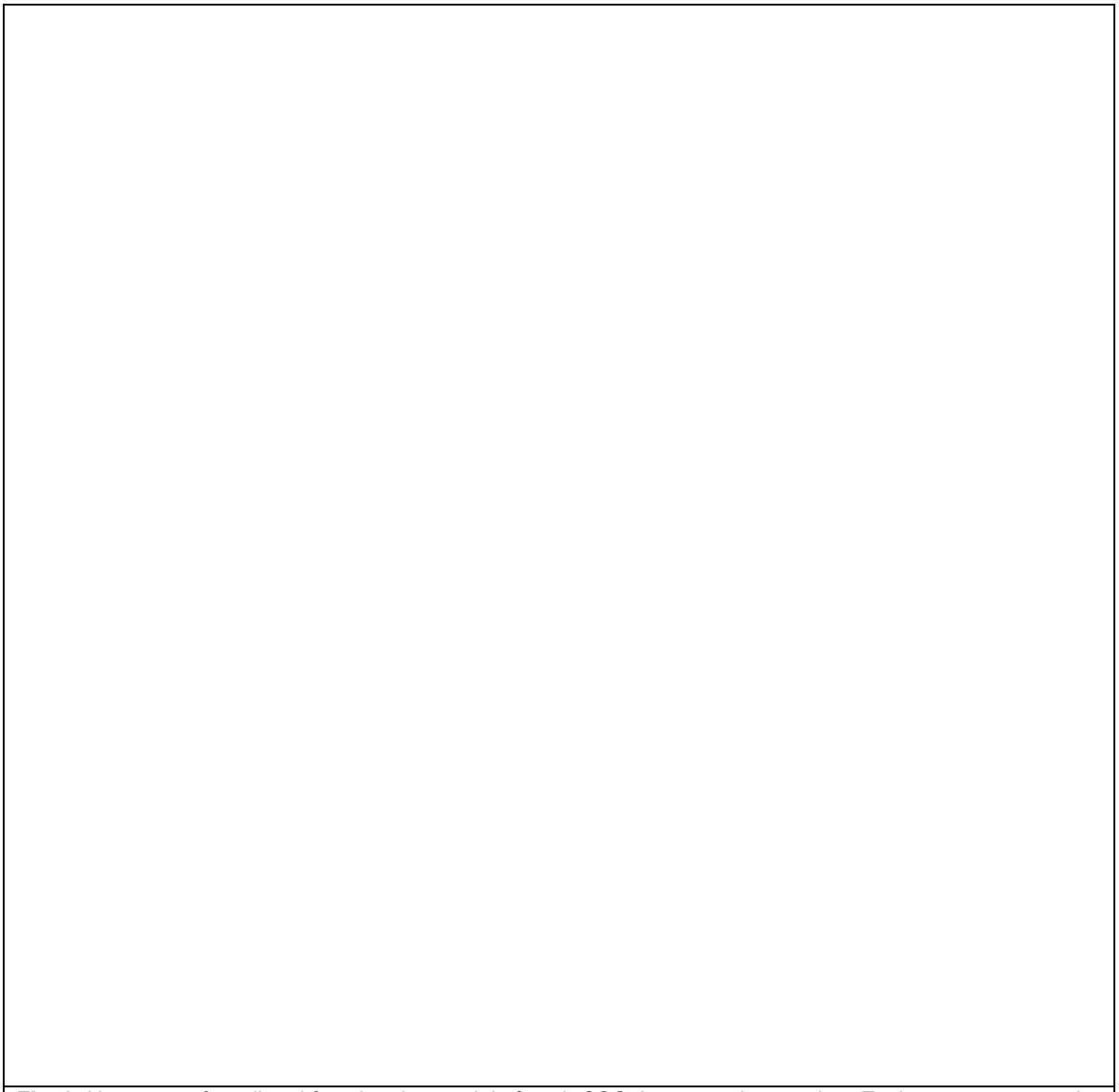

Fig. 8. Heat map of predicted functional potential of each CSC-A community member. Each row represents the functional enrichment or depletion of a life-history trait. Rows are split into 5 groups based off of hierarchical clustering. Red cells indicate enrichment of a trait in an organism and blue indicates depletion. Values are trait counts normalized to genome length. The bar on the left side of the heatmap indicates which category of life-history trait each row corresponds to.

We mapped KEGG ontology ID's to a total of 10,368 loci in the CSC-A metatranscriptome. Comparing communities with and without *C. flaccumfaciens*, (Locus ID prefix of IHGJAF) we identified a total of 885 highly differentially expressed genes (DEGs) (-3 < Log2FoldChange > 3 and an adjusted *p*-value of < 0.05), in three samples across a 48-hour time course (0 – inoculation, 24, and 48 hours). We did not recover evidence of any transcriptional changes during removal of

C. flaccumfaciens directly relating to urea or MICP related metabolic functions, suggesting that *C. flaccumfaciens* may not be heavily involved in these specific processes. We observed no significant gene upregulation in the 24 hour sample, with all DEGs exhibiting decreased expression as a function of *C. flaccumfaciens* loss and mapping to the *R. qingshengii* (Locus ID prefix of KXIUOE) transcriptome. Of these, statistically significant DEGs coded for transferases like the antigen biosynthesis glycosyltransferase and degradation enzymes for valine, leucine, threonine, and isoleucine, and carbonic anhydrase. Across the 24- and 48- hour timepoints, other significant DEGs coded for catalytic enzymes, and transport proteins. At the 48-hour time point, highly expressed genes in the absence of *C. flaccumfaciens* were mostly associated with *B. toyonensis* and mapped to functions such as maintaining cell survival, metabolic regulation, phosphotransferase enzymes, and other degradation catalysts. Other significant DEGs at 48 hours were mapped to ribosomes and DNA forming proteins in *B.toyonensis*, *Microbacterium*, and *R. qingshengii*.

However, when *R. qingshengii* was removed from CSC-A, we identified a cumulative 9,009 DEGs when comparing two timepoints to their respective control condition—more than ten times as many genes were identified during the absence of *C. flaccumfaciens*. Removing *R. qingshengii* resulted in strong upregulation of *B. toyonensis* genes coding for stress, regulatory and stabilizing responses, bicarbonate conversion and carbonic anhydrase, kinases and other catalysts, and zinc transport proteins in the 24-hour timepoint. In the absence of *R. qingshengii* at this same timepoint, statistically significant downregulated DEGs were all associated with *Microbacterium* (Locus ID prefix of PGEDEG), coding for flagellar biosynthesis and locomotion, and protein synthesis inhibition genes. At the 48-hour time point, significant DEGs all belonged to *B. toyonensis* and included thioredoxin genes, transcriptional regulators, and arginosuccinate synthase. Given the significant impact of the removal of *R. qingshengii* from the CSC-A community on ensuing gene expression, we decided to further explore the role *R. qingshengii* in the context of MICP.

At least one community member, *R. qingshengii*, was predicted to have urea degradation capabilities via hydrolysis. This process and its ensuing precipitated product are likely to result in altered metabolic requirements for growth, due to the increased pH and resulting breakdown products over time. To better understand the effects of added urea to the functional output of CSC-A, we used the likelihood ratio test, paired with cluster analysis, to identify sets of co-expressed genes exhibiting significant changes in expression over 3 sampling points using meta-transcriptomics profiles from the complete CSC-A grown in either base B4 media or B4 with urea (B4UZN) added. We identified multiple clusters containing DE co-expressed genes from all community members and tested each for KEGG module enrichment. We identified 11 total clusters of significantly co-expressed genes, 6 of which contained a larger number of genes from specific KEGG modules than expected by chance (**Figure 9A-H**). 48% (1518) of the DE genes came from *R. qingshengii*, followed by *C. flaccumfaciens* 1080 (35%), *Microbacterium* 342 (11%), and finally *B. toyensis* 192 (6%). Clusters 2 (128 genes), 9 (139 genes), and 12 (57 genes) decrease in expression over sampling points, and are dominated by *R. qingshengii* genes (77%), and which contain amino acid metabolism modules such as methionine salvage, de novo purine biosynthesis from glutamine, as well decreased expression of meromycolic acid biosynthesis and central metabolism modules such as the Calvin and Citrate cycles. Groups 4 and 5 contained 175 genes which exhibit increasing expression by the last time point in B4UZN media but decreased expression in control B4 media. These groups contained mostly *C. flaccumfaciens* genes related to amino acid metabolism overlapping with group 1, energy modules such as the pentose phosphate pathway, and gluconeogenesis. Finally, group 11 contained 23 genes split relatively equally among community members related to the denitrification KEGG module that converts

nitrate to nitrogen. This group exhibits no change in expression during growth in urea, but significantly decreases over time in control media.

Taxa specific metabolomics identifies differences between community and individual metabolome profiles

We identified metabolites that were potentially consumed, precipitated, and exchanged between members of the CSC-A consortia when grown in urea-enriched (B4UZN) media. To assess this, we made use of an individual well and shared reservoir experimental setup where single species cultures were inoculated into individual cells, with the floor of the cell made of a semi-permeable membrane rather than plastic. Wells are then connected to each other through a shared reservoir at the bottom of the plate, allowing for metabolite and nutrient transfer while maintaining segregation of species. Metabolite samples from individual wells, when compared to the uninoculated control media, helps compile metabolic profiles for each individual species. Profiles were also compared to the shared reservoir to determine species-specific enrichment or depletion of individual metabolites.

Principal Component Analysis comparing individual profiles to those of uninoculated control media and the shared well (**Figure 10A**) indicated a significant change in metabolite composition during community growth, with the first principal component explaining 79% of the variation in the top 500 most variable metabolites. When removing the uninoculated control media from assessment, metabolic profiles from *C. flaccumfaciens* were located closest to the shared reservoir samples, followed by *R. qingshengii* and *Microbacterium* (**Figure 10B**). Along the first and second principal components, *B. toyonensis* contributed the only set of profiles which were distinctly separate from the shared reservoir samples.

The top eight significantly enriched metabolites (when contrasted to a media control of B4UZN) in the ‘shared’ well after a five-day growth period included Camphor-10-sulfonic acid, N-(5-acetamidopentyl) acetamide, indole-3-lactic acid, 1,3-Cyclohexanedicarboxylic acid, 4-Hydroxy-6-methyl-2-pyrone, 3,5-Dichlorosalicylic acid, 4-Hydroxyphenyllactic acid, and monobutyl phthalate—most of which are likely metabolic byproducts (Table 4). The top eight metabolites significantly depleted were sn-Glycero-3-phosphocholine, nicotinamide, val-thr, val-val, d-xylose, 2,3-Naphthalenedicarboxylic acid, L-Asparagine, and arginine—many of which are amino acids or amino acid dipeptides involved in the biosynthesis of proteins or organic compounds. These likely represent the metabolites that CSC-A is producing or consuming, respectively, at the community level.

Fig. 9. Cluster analysis of temporally co-expressed genes during growth in urea. Left: each group represents a set of co-expressed genes across three timepoints. Bold lines across time points are general additive model fits for each group across time: 0: Inoculation, 1: 24 hour timepoint, and 2: 48 hour timepoint. Right: Dot-plot indicating significant KEGG module set-overrepresentation for each cluster. Dot size indicates the number of genes within the gene group that belong to each module, and color indicates the enrichment value.

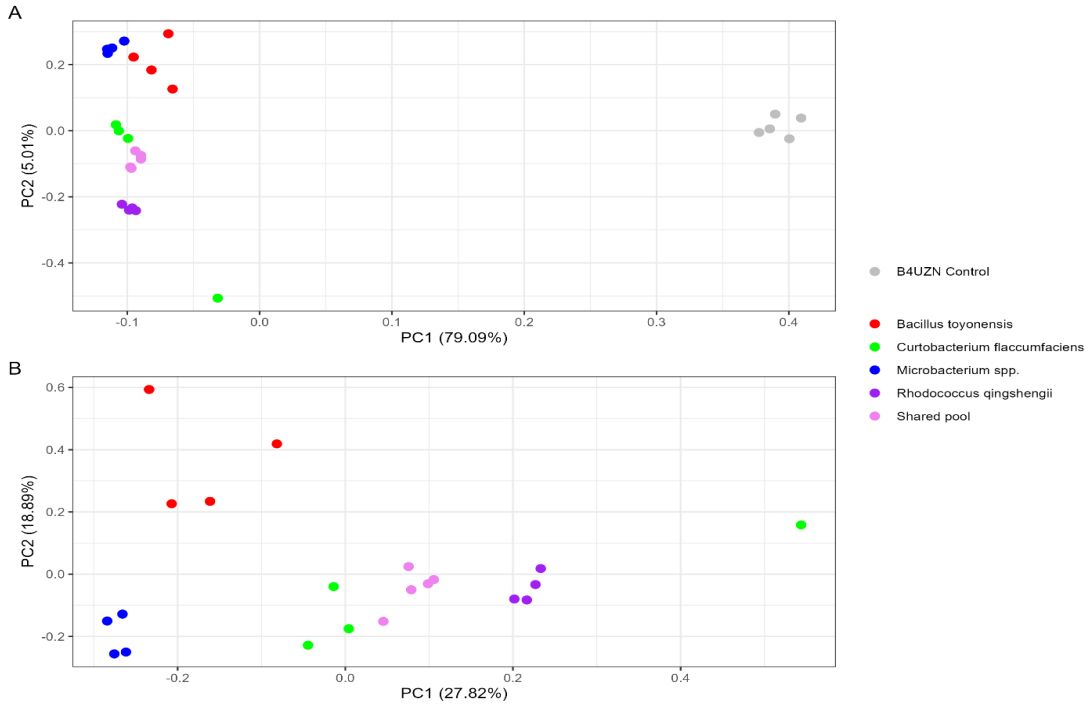

Fig. 10. Principle Component Analysis (PCA) plot illustrating metabolite expression between CSC-A members with B4UZN control media (A), and without control B4UZN media (B) for contrast. The stark difference in variance

between the control group (A) to other metabolite expressions (CSC-A species and shared pool) suggests a strong distinction between metabolite samples from the control group and all other groups.

We next tested for enrichment and depletion of metabolic byproducts during growth in comparison to an uninoculated control well, assessing at a *p-adjusted* value of 0.05. Ubiquitous across most species-specific metabolite profiles was the depletion of sn-Glycero-3-phosphocholine and D-(+)-Trehalose, and the enrichment of 4-Hydroxy-6-methyl-2-pyrone. Though *B. toyonensis* was the producer of most of these differentially enriched metabolites, the metabolites with the highest enrichment-Camphor-10-sulfonic acid (Log2Fold = 5.156) and 2,3-Naphthalenedicarboxylic acid (Log2Fold = 5.012), were associated with *Microbacterium*. *R. qingshengii* wells had the highest depletion of the metabolite sn-Glycero-3-phosphocholine (Log2Fold = -5.194). While there were significant differences in enrichment between individual wells and the shared reservoir, differences were lower in magnitude than what was observed versus the uninoculated control sample; the highest enriched metabolite was the dipeptide Ile-Leu (Log2Fold = 1.805) during growth of *B. toyonensis*, and the most depleted was the demethylation byproduct and biosynthetic precursor S-Adenosyl-homocysteine (Log2Fold = -2.349) in the *Microbacterium* well. Of the 10 metabolites with the strongest enrichment across the community, 8 were within the organic acids and derivatives KEGG superclass, while 5 of the top 8 depleted metabolites belonged to the nucleosides, nucleotides, and analogues superclass, indicative of categorical DE of metabolite classes.

CSC-A members utilize distinct methods for metabolizing urea degradation byproducts and mitigating stress, driven by R. qingshengii and B. toyonensis.

Once we identified changes in gene expression and metabolite profiles during growth in urea-rich environments, we integrated our results to identify functional enrichment with multiple forms of evidence. For each species, we searched the KEGG reactome for reactions with at least one differentially enriched orthologous gene and one differentially enriched metabolite. These results were cross-referenced with the results of an expression-based KEGG pathway gene set enrichment analysis (GSEA). We identified 29 reactions supported by both transcriptomic and metabolomic datastreams from *R. qingshengii*, 26 for *B. toyonensis,* 16 for *Microbacterium*, and 2 for *C. flaccumfaciens* (Table 5). *R. qingshengii, B. toyonensis,* and *Microbacterium* all shared decreased expressions of the succinate:quinone oxidoreductase reaction of the TCA cycle, leading to increased succinate.

In *R. qingshengii*, we observed 19 differentially expressed KEGG pathways via GSEA. The ABC transporters pathway exhibited positive enrichment (Table S3), with strong upregulation of the K11962, K11960, and K11961 orthologs coding for multiple subunits of the urea transport system, as well as the Sulfur metabolism pathway, though no reactions with paired metabolite data were associated with this pathway. *R. qingshengii* also possessed the largest set of reactions with both transcriptomic and metabolic evidence, with multiple examples of nitrogen metabolism-related reactions acting on the major hub molecule L-glutamine, which was depleted during *R. qingshengii* growth in urea. This resulted in significant repression of multiple glutamine-associated KEGG pathways, such as the TCA cycle (ko00020), Biosynthesis of amino acids (ko01230), and Glyoxylate metabolism (ko01100). We observed upregulation of the dTDP-4-amino-4,6-dideoxy-D-galactose:2-oxoglutarate aminotransferase involved in producing nitrogen containing cell membrane components, and downregulation of multiple other reactions with glutamate as a reactant, such as (2S)-2-amino-4-deoxychorismate: L-glutamate aminotransferase, which produces glutamine and chorismate from glutamate and (2S)-2-amino-4-deoxychorismate. We also identified upregulation of 3-xanthine-dehydrogenase enzyme subunits mapping to the KEGG orthologies for *yagRST*, which bi-directionally converts xanthine to uric acid and xanthine to

hypoxanthine alongside increased xanthine (log2FoldChange 2.306408, p adjusted = 4.438273e-06) and hypoxanthine (log2FoldChange = 1.205648, p adjusted = 4.438273e-06) abundance during growth in urea. Similarly, GSEA analysis of *B. toyonensis* expression identified downregulation in the glyoxylate and dicarboxylate, and 2-oxocarboxylic acid metabolism KEGG pathways, which mapped to multiple related reactions with expression and metabolomic evidence. Of the 23 pathways differentially enriched in *B. toyonensis*, all were downregulateddepleted.

GSEA of *Microbacterium* expression identified 12 KEGG pathways, including enrichment of the two-component system pathway, increasing expression of regulator genes responsive to hypoxia and redox stress. *Microbacterium* also produced multiple reactions related to glutamate metabolism. These reactions include a decreased expression of the L-glutamate: ammonia ligase (ADP-forming) reaction, which incorporates ammonia into glutamate, and increased expression of multiple transaminase reactions resulting in a depletion of the L-glutamine metabolite. *C. flaccumfaciens* only yielded 2 reactions: decreased D-Xylose driven by the conversion of D-Xylose to D-Xylulose, and decreased expression of the proline utilization regulon repressor driving increased levels of proline. The only pathway enrichment detected for *C. flaccumfaciens* was significant depletion of the ABC transporter pathway.

After the analysis of each individual CSC-A member, we projected the entire set of community reactions as a DE metabolite-reaction network during growth under urea-rich conditions (**Figure 11**). Two or more community members contributed to 4 subnetworks of the KEGG reaction network. Decreasing Phenylpyruvate (C00166) and increasing Succinate (C00042) compounds exhibited the largest network degree (10) and associated set of reactions, with a set or reactions shared among *R. qingshengii*, *B.toyonensis*, and *Microbacterium* connecting Succinate to Fumarate. L-Phenylalanine (C00079) and L-Glutamate (C00025) and a large set of reactions both decreased during growth in urea. Reactions and compounds associated with these subnetworks belonged to 23 amino acid, cofactor and vitamin, and carbohydrate metabolism KEGG pathways. Multiple amino acids such as L-proline (C00148), L-Cysteate (C00506), and Glycine (C00037) were all increased during growth in urea, though had low connectivity in the network.

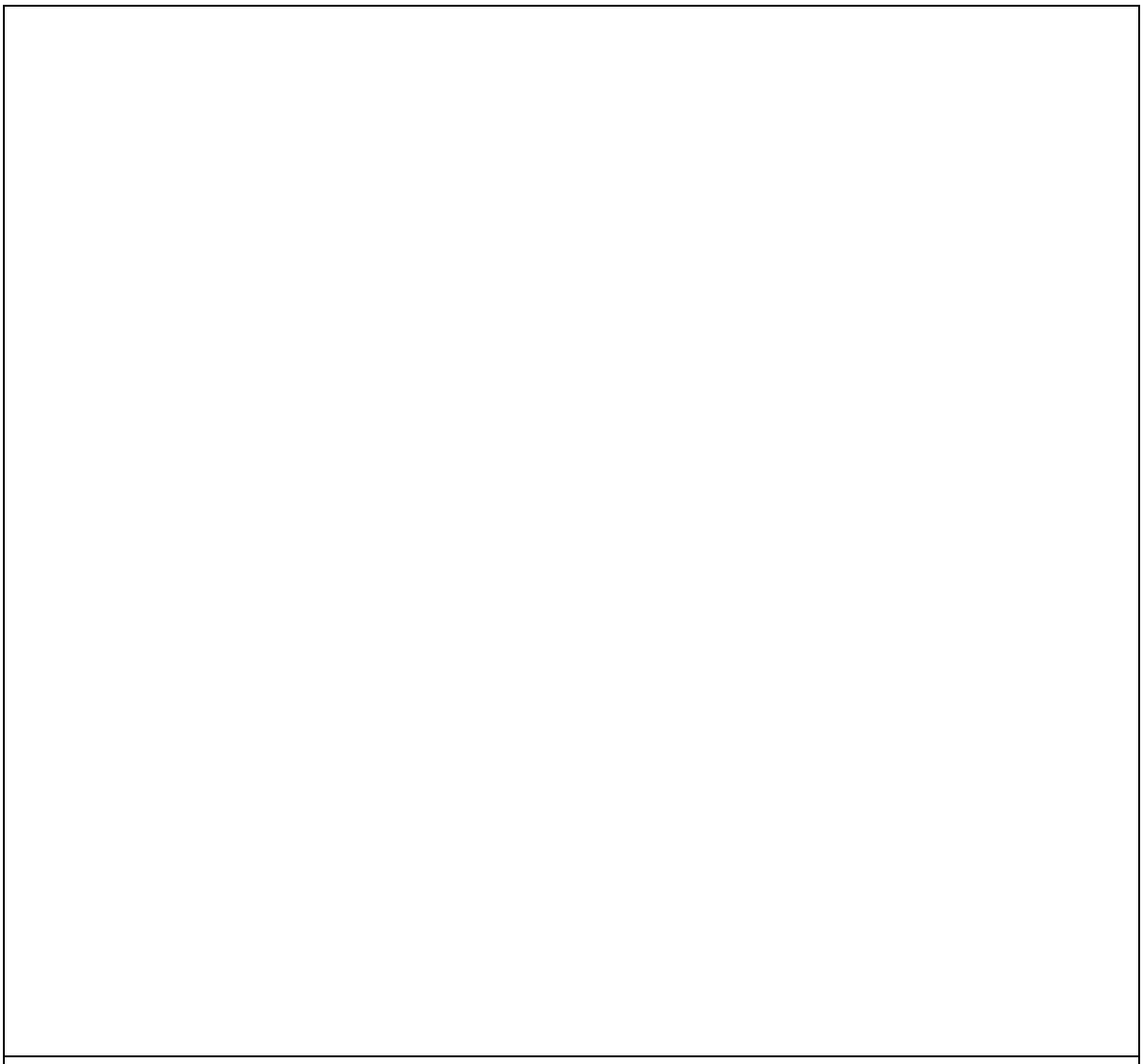

Fig. 11. Community metabolite-reaction network of the dual evidence CSC-A reactome. Nodes represent KEGG compounds and edges represent KEGG reactions with a DE metabolite and at least one DE KEGG ortholog expression. Glow signifies DE, with green being enriched and orange being depleted. Node size indicates network degree. Nodes are colored by the KEGG pathway they are a connected to, and edge line type corresponds to the individual community member the evidence comes from.

As succinate and arginine were major nodes in our interaction network we tested whether these metabolites could enhance carbonate production when added to B4UNZ media. We found that the addition of arginine did lead to a 2.4-fold increase in carbonate production but only at one out of three tested timepoints (48 hours after the start of the experiment) (**Figure 12**). Succinate addition led to increased carbonate production at both 48 (2.4-fold) and 72 hours (1.48-fold) after the start of the experiment. This finding is a key link between our modeling data and laboratory production of $CaCO_3$, showing that altering how we cultivate CSC-A based on model outputs can further enhance phenotypes of interest, increasing our ability to predict and control them.

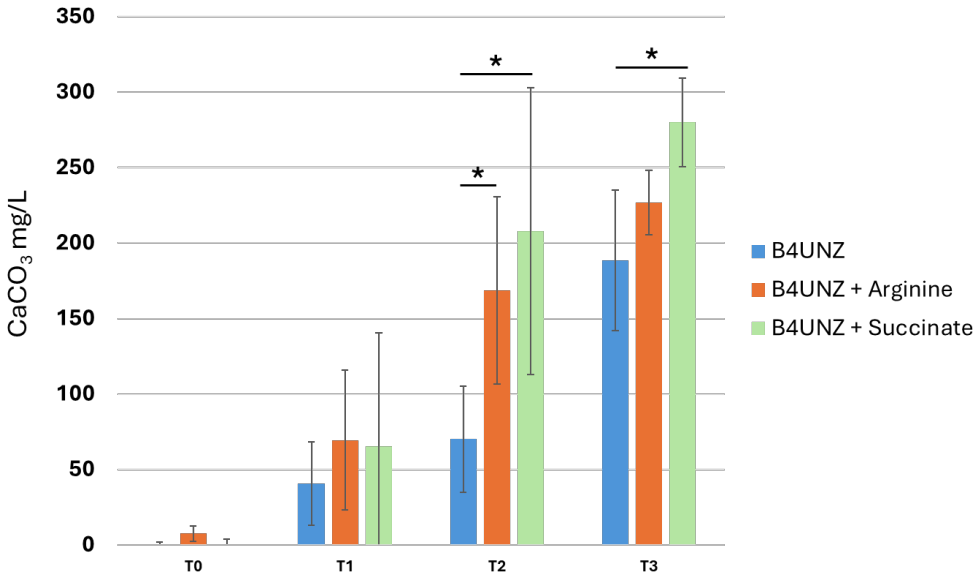

Fig. 12. Production of $CaCO_3$ by CSC-A during cultivation with added metabolites. Amount of $CaCO_3$ is shown in the y-axis and timepoints (T0 = 0 hours, T1 = 24 hours, T2 = 48 hours, T3 = 72 hours) are shown on the x-axis. * indicate p-values less than 0.05.

3.0 Discussion

Here we describe the development and analysis of a consortium of soil bacterial species which have a range of phenotypes related to calcium carbonate production. We show that constituent species of CSC-A can drive the production of $CaCO_3$ but that production by the combined growth of all members, (CSC-A), exceeds the sum of $CaCO_3$ found with individual species. We also show that this consortium is stable across time and that no one species outcompetes the others.

Prior work has identified some individual species and some of the enzymatic processes that are at the center of MICP in soil. However, no species that carries out MICP exists in a monoculture in native ecosystems. Metabolic cross talk and interspecies support is a major driver of soil microbiological functions (Morris et al. 2013; Xinyu Zhu et al. 2020). Because of this, it is equally important to understand how a community of microbial species interacts to carry out carbonate formation as it is to understand the individual species involved. The development of CSC-A allows to ask and answer questions related to community production of $CaCO_3$. Our results, especially **Figure 6,** clearly show that CSC-A produces a higher amount of carbonate than the sum of the individual species, the whole is greater than the sum of its parts, pointing to interactions within CSC-A being critical to carbonate production by this consortium. There are several possible ways that interspecies interactions could increase $CaCO_3$ in CSC-A. Based on the measurements of individual species we hypothesize that most of these interactions flow through *Rhodococcus*, the major driver of $CaCO_3$ production when species are cultivated separately. One possibility is the production of urea by another species that is then passed to *Rhodococcus* for enzymatic processing by urease. *Rhodococcus* members, including *Rhodococcus qingshengii*, the species used in CSC-A, have been found that have urea transporters (Letek et al. 2010; Xu et al. 2007) and while *Rhodococcus* may be able to synthesize its own urea as well, additional urea from other members of the consortium could enhance carbonate production and $CaCO_3$ precipitation at the consortium level further. Future studies examining each member of CSC-A individually using a metabolomic approach could delineate which species make urea for community consumption. It is also possible that other metabolites, not related to urea or carbonate production, could define synergistic interactions between species. Our amplicon analysis shows that many of the species have relatively even abundances when co-cultured suggesting positive interactions, or at least the absence of strong competition. If other species can support the growth of *Rhodococcus* in a general way (aside from urea transfer), this could lead to faster growth of *Rhodococcus* and enhanced $CaCO_3$ precipitation. Our analysis of CSC-A included only the full consortium, not subset or pair wise comparisons. However, it is possible that the increased $CaCO_3$ production we see with CSC-A is not a function of the complete community but only of a specific set of interactions between *Rhodococcus* and another member. Pairwise incubations between all members, but especially *Rhodococcus*, could test this hypothesis. In addition, our planned next steps include gathering species specific multi-omic data including metatranscriptomics. Knowledge of what specific processes each member expresses during growth in CSC-A will also help us identify pairwise interactions, identifying where $CaCO_3$ production requires CSC-A as a whole or just one or two constituent members. It is also possible that species that show little carbonate production in monoculture may increase MICP when cultured within CSC-A. Phenotypes are not static and can shift due to the surrounding environment and taxonomies (Heyse et al. 2019; Jean-Pierre et al. 2023; Ryan McClure et al. 2023; Zuñiga et al. 2019). Further analysis using pairwise combination experiments (Ryan McClure et al. 2023) or metatranscriptomic analysis (Ryan McClure et al. 2022) will be critical in revealing which species produce the most $CaCO_3$ within CSC-A.

The conclusions above would not have been possible without the development and analysis of our reduced complexity consortium, CSC-A. Such model consortia have also been useful in exploring other aspects of soil microbiology (R. McClure et al. 2020; Lozano et al. 2019).

Development of such consortia usually proceeds along two separate routes. Either consortia can be made from combinations of individual isolates (Herrera Paredes et al. 2018; Shayanthan, Ordoñez, and Oresnik 2022) or they can be made through cultivating field samples in the lab and allowing for the emergence of an interacting set of microbes using passaging and dilution (R. McClure et al. 2020; Zegeye et al. 2019). Species comprised of individual isolates have the advantage of greater control and knowledge regarding the make-up of the consortium, however, combined species may not interact, either positively or negatively, meaning that conclusions may not be as translatable. In contrast, consortia that are allowed to emerge based on existing interactions between bacterial species, those whose constituent members are not chosen by the user, have a better chance of representing native interactions, or at least, interactions representative of the conditions that they were cultured under, but the complete taxonomic and genomic potential of the community is difficult to determine and detailed experiments on individual members is not possible. Here, we take a combined approach where consortia are allowed to develop through several weeks of passaging followed by isolation of species and recombination. This maximized our chances of generating a consortium reflecting true interactions while also giving us a great deal of control over community makeup, experimental design and data related to the role of each species.

We noted if there was a pH change or the production of white precipitate (later confirmed to be $CaCO_3$) every week and found that, especially in early weeks, there was a great deal of variability from week to week when looking at pH changes or precipitate formation. This is despite the fact that this is a closed system, and the introduction of new species is not possible. Since we re-passaged the microbes each week, we were essentially allowing a new consortium to assemble with each transfer. Several studies have examined the role of stochasticity in consortium or community assembly. One recent review laid out four elements of community assembly (Zhou and Ning 2017), of these selection (ecological factors that alter community structure due differences in fitness) and drift (species identity with regard to the relative abundance of all species in the community) apply most strongly to the development of CSC-A. According to the authors, selection is inherently not stochastic while drift inherently is stochastic. Stochastic effects of community drift may be a main driver as to why carbonate production and pH changes varied from week to week even in the same medium and community replicate. Slightly different changes in drift and, possibly, selection, led to slightly different consortia , the downstream effect of which was major changes in community phenotypes ($CaCO_3$ production). These experiments emphasize the need to cast a wide net when attempting to develop communities with certain characteristics and allow time for communities to stabilize. Both time and diversity of starting conditions are needed to counteract the inherent stochasticity of community development and increase the chances of finding a community that fits the needs of the experiment. Other studies have also found that stochasticity is a main driver in community assembly and even that pH changes, a major factor in these experiments specifically, can significantly affect stochastic assembly of communities (Tripathi et al. 2018; N. Liu, Hu, et al. 2021).

Despite the stochasticity we see in the consortia phenotypes across the range of passaging, the final consortia had many of the same species. This suggests that the difference in phenotypes that we see is not just a reflection of taxonomic differences in the consortia but also a function of which genes and processes are being expressed at the consortium level. Such phenotypic outcomes are the result of a complex set of inputs and other studies have also found that microbial communities of similar taxonomies can have widely different sets of expressed genes and functions (Naylor et al. 2020). We also consistently saw the emergence of the five species used in our final CSC-A, despite differences between media types and replicates. This strongly suggests that these species have a suite of interactions that allows them to grow together (they emerge repeatedly from the native soil microbiome). This is another argument in favor of multiple evolutions with similar or identical conditions in such experiments. If the same set of

species consistently emerge, despite the random chance that is a function of these enrichments, this is a strong argument that they should be examined further. We hypothesize that these interactions are one of the reasons why we see significantly higher amounts of $CaCO_3$ in CSC-A versus any of the constituent species or even the combination of all species.

The use of microbial communities to sequester carbon in soil has been considered as a carbon mitigation strategy for several years (Y. Wang, Konstantinou, et al. 2023). However, there are significant hurdles that stand between development of a community in a laboratory setting and application of this community, or the fundamental knowledge gained, to the field (Mason et al. 2023; Fierer and Walsh 2023). Here we are adding significant carbon to the medium in the form of B4 (containing tryptone and yeast extract) as well as the urea itself. In addition, nickel is being added as well, a well-known urease cofactor (Mazzei, Musiani, and Ciurli 2020). We see less $CaCO_3$ under other kinds of medium (e.g. B4) which shows that available metal ions and nutrients have major effects on $CaCO_3$ production. Such knowledge could help us target downstream application studies, focusing on systems with free calcium or nickel and higher inputs of urea (from fertilizer for example).Addition of carbon also means there is likely significant respiration from the community, depending on carbon use efficiency (Adingo et al. 2021). Stored carbon in the form of carbonate (or microbial biomass and necromass) must exceed the amount respired for long term storage to be feasible. In addition, the added carbon in these experiments speaks to the possibility that there may not be enough nitrogen or carbon sources in native soil to stimulate robust growth and thus carbonate formation. Pairing species driving $CaCO_3$ production with plants whose exudates could be a carbon and nitrogen source, especially those that have deep root systems (Lamb et al. 2022), will be a critical link to capturing carbon directly from the atmosphere, putting it into soil as exudates or litter and storing it long term via MICP deep in the soil. Sufficient minerals must also exist in the soil to lock the carbonate into $CaCO_3$, or other forms that are inaccessible to metabolism, and the soil pH must be high enough (~7.5 to 8) for the $CaCO_3$ to precipitate. Finally, the work we show here focuses on a very simple and artificial system compared to the complete soil microbiome. Our discoveries must first be confirmed in more complex and natural environments, linking our laboratory and field work, before we take the next steps to modify these systems to harness them for carbonate production.

Challenges remain in harnessing the soil microbiome to store carbon long-term, but a deeper understanding of the community-level processes involved is critical to addressing these challenges. The development and analysis of CSC-A will allow the scientific community to start to fill these knowledge gaps. We will be able to explore the role not only of individual species, but also of the interactions between them and how these effects change with shifts in carbon source, pH, and environment (liquid cultivation vs. back in the native soil). As we gather more knowledge on how species interact to sequester carbon, we will be better equipped to implement measures to enhance the formation of inorganic carbon in the soil. This could include using knowledge gained to drive the native soil microbiome to carry this out, or through the direct application of carbon capturing communities to soils, in a manner similar to what has already been seen over the past decades with microbial communities that have revolutionized agriculture and plant growth.

CSC-A exhibits a broad range of growth rates and metabolic potential, utilizing unique methods for environmental resistance and nutrient acquisition. This results in specific niche roles played by *R. qingshengii*, *B. toyonensis,* and *Microbacterium* during growth in urea. This observation is juxtaposed with *C. flaccumfaciens*, which had the lowest number of DEGs, a small impact on the community transcriptome, and a metabolome most like the shared reservoir. The relative sparsity of *C. flaccumfaciens* reactions mapped back to the transcriptome and metabolome also corroborates this. The life history trait analysis identified *C. flaccumfaciens* as having the longest MGT and highest OGT, which suggests that it may be outcompeted by faster growing community members whose OGT is more optimized for the temperature of lab experiments. *C. flaccumfaciens* are a widespread and “cosmopolitan” taxon, with large genomic

potential for carbohydrate degradation, which we observe in our life history analysis. *C. flaccumfaciens'* specialization in complex carbohydrate degradation may not be well optimized for *in vitro* lab experimentation with pre-digested, complete growth media. There was some evidence of increased co-expression of multiple sets of *C. flaccumfaciens* genes related to amino acid and central metabolism, potentially indicating the end of lag phase starting to occur at the 48-hour timepoint. Future studies in minimal media supplemented with complex carbohydrates, such as cellulose or chitin as they are naturally occurring sources in adjacent soil environments, could tease out environmental scenarios optimal for *C. flaccumfaciens* growth in CSC-A.

Background on the MICP process suggests that in a high urea environment, MICP will primarily proceed through the degradation of urea into ammonium and carbonic acid. Though *Bacillus spp.* have been observed degrading urea and contributing to MICP, *R. qingshengii* was the only member predicted to be capable of urea degradation via urease, positioning it as a keystone species facilitating urea degradation within the consortium during MICP. Pathogenic *Rhodococcus equi* are known to degrade urea via urease, where it plays a role as a known virulence factor. Similarly, CSC-A's *B. toyonensis* and *Microbacterium* both displayed genetic potential for metabolic activity characteristic to their genera, such as protein homeostasis and degradation via ATP-dependent proteases and redox stress tolerance through two-component regulatory systems. We hypothesized that these unique metabolic abilities would naturally result in the division of labor, distributed signal processing, and temporal dynamic properties commonly implemented in engineered microbial consortia for bioproduction. The sets of temporally co-regulated gene groups with unique KEGG module enrichment targeting methionine salvage or conversion of glutamine to UMP dominated by one community member supports this hypothesis. Cluster 11, which carried denitrification genes was more evenly distributed across the community, suggesting that nitrification stress is a significant threat to individual member growth, and each implement strategies to mitigate this.

As suggested by Malard and Guisan, genes of a metatranscriptome are dependent on and reflect characteristics that define where an organism can realistically survive, i.e. their specialized niches. We believe that some of our data supports the understudied, complex theory of specialization for functional niches, as has been characterized in pathogenic bacteria for host subversion and to a lesser extent, soil bacteria in new habitats with different resources. For example, only 885 significantly DEGs were identified in the absence of *C. flaccumfaciens*—a fraction of those. This suggests that this member either contributes a small share of total niche specialization in the consortium, or conditions are not conducive to encourage growth. However small its presence, its absence seemed to have impacts on the metatranscriptome. When *R. qingshengii* genes were downregulated in the absence of *C. flaccumfaciens*, they were associated with metabolic functions such as the degradation of sulfur containing groups, and amino acid degradation, suggesting that *C. flaccumfaciens* contribute some metabolic products *R. qingshengii* and other CSC-A community members utilize. Under these same conditions, *B. toyonensis* DEGs coded for peptide and nickel protein transporters, repair, and metabolic regulation, metabolic functions less likely to result from community interaction. We hypothesized that this expression regime in the absence of *C. flaccumfaciens* results in decreased growth and degradation of amino acids in *B. toyonensis* at earlier timepoints, which then switches to upregulating protein synthesis and metabolism genes at the last sampling point.

Though the removal of *C. flaccumfaciens* seemed to shift the functional niches of CSC-A members, as R. *qingshengii* was the only consortia member predicated to be capable of degrading and transporting urea inside the cell, we expect it act as a keystone species during growth in urea. Therefore, while removal of *R. qingshengii* from the CSC-A consortia would inhibit urea and nitrogen degradation, we expected other indirect effects on community metabolism and niche shifting. As anticipated, the absence of *R. qingshengii* resulted in far more metabolic DEGs

than removing *C. flaccumfaciens*; a collective 9,009 DE versus 885, respectively. Unlike in the absence of *C. flaccumfaciens*, the number of DEGs increased at the 48-hour timepoint. This suggests a sustained metabolic effect on CSC-A, further supporting the hypothesis of niche reorganization occurring to compensate for the absence. This is further supported by the functions of some of the most upregulated genes in *B. toyonensis* in response to loss of *R. qingshengii*, such as carbonic anhydrase and cyanate lyase, which we previously mentioned are alternative methods for precipitating calcium carbonate and producing ammonia. While the possibility that these MICP-central enzymes are being activated was not explored in this experiment, their upregulation of these enzymes' genes potentially validates recent research efforts that emphasize their utilitarian potentials for enhancing MICP.

Arginosuccinate synthase was also highly expressed by *B. toyonensis*, and, unlike during the full community growth in urea, where other arginine related reactions were favored. Removal of *R. qingshengii* also resulted in significant lowered expression of many flagellar biosynthesis and protein synthesis genes from *Microbacterium.* This information suggests that in the absence of the CSC-A's strongest urea degrading member, *B. toyonensis*'s ecological niche expands, taking over nitrogen metabolism and MICP activities, potentially at the cost of restructured arginine metabolism and *Microbacterium* metabolic activity. This expansion from realized niche breadth to fundamental niche breadth has also been observed in soil environments during lower biotic pressure.

Metabolite profiles indicate that when grown in B4UZN media, CSC-A members process this growth media into a wide array of products. Ammonia, the byproduct of urea degradation, is a preferred nitrogen source for incorporation into amino acid metabolism. We also observed +4-Hydroxyphenyllactic acid, L-asparagine, and nitrogen metabolite 2-((7-acetamido-1,2,3-trimethoxy-9-oxo-5,6,7,9-tetrahydrobenzo[a]heptalen-10-yl)amino)-N-(2,4-dimethoxyphenyl)-4-(methylthio)butanamide, significantly enriched among all four CSC-A members. Metabolites significantly enriched within the shared pool consisted mostly of branch chained-amino acids such as Phe-Val and Leu-Tyr. MICP has been shown to modulate cell membrane characteristics by upregulating branched chain amino acid and fatty acid biosynthesis. Notably, the single most highly enriched metabolite among the shared pool associated with *Microbacterium* is urocanic acid, a byproduct of L-histidine degradation typically found in urine and sporulating bacteria. Depletion of S-Adenosyl-homocysteine, involved in methionine synthesis for translation, and Nicotinamide, necessary for synthesizing metabolism cofactors NAD and its derivatives, across all four individual pools as well as the shared pool, suggest that CSC-A consortium is actively metabolizing and growing throughout the duration of the study (Figures 3, 4). Notably, *C. flaccumfaciens* did not produce a significant change in the detectable metabolites in the shared pool, providing further evidence that it may not be metabolically active enough to produce a detectable change in chemical concentration. sn-Glycero-3-phosphocholine, important as a cell membrane component and as a biocatalyst when hydrolyzed, was depleted in the individual taxa wells relative to the media control.

Aside from urea, other studies have determined that Ca^{2+} and dissolved organic carbon concentrations, environmental pH, and the availability of nucleation sites were all key factors influencing MICP. *C. flaccumfaciens* and *Microbacterium* were both predicted to hold the largest complements of inorganic transport genes, which are important for regulating the concentration of Ca2+ in the cell at low levels while allowing for survival in high Ca2+ environments where MICP is likely to occur. Multiple reports suggest that Ca2+ transport is linked to active MICP, either by playing a significant role in mineralization or by promoting a localized increase in pH due to proton uptake, thus creating microenvironments conducive to MICP. Surprisingly, GSEA analysis of the transcriptome identifies significant repression of the Ca2+ pathway in *C. flaccumfaciens*, with simultaneous enrichment in *R. qingshengii*, a community member not predicted to have as great

a complement. We hypothesize that specific members of CSC-A within the consortium have adapted to providing for this task.

MICP is a process underpinned by complex network of interconnected gene expression and metabolite usages within a genetically diverse soil microbial consortium. We found that integrating the meta-transcriptomics and metabolomics data gave us the most comprehensive view of metabolic integration during CSC-A growth in urea. The identified reactions confirm our prediction that metabolic flux through members of the community span multiple KEGG pathways and ecological niches, except for *C. flaccumfaciens*. *R. qingshengii* and *B. toyonensis* had large reaction sets, indicative of their important roles during urea degradation in CSC-A. Glutamate was central to one of the largest subnetworks of reactions, and cross-pathway glutamate metabolism were identified as highly modulated during growth in urea. with substantial evidence for metabolic activity in this subnetwork from *R. qingshengii*, *Microbacterium,* and *B. toyonensis*. *Microbacterium* showed increased expression of multiple aminotransferase reactions acting on or with glutamate, while *R. qingshengii* and *B. toyonensis* exhibited more heterogeneous expression of glutamate reactions. The temporal co-regulation analysis identified a group of genes largely from *R. qingshengii* with decreased expression of the de novo purine biosynthesis KEGG module which converts glutamine to IMP. This indicates that the metabolic activity involved in the glutamate network occurs mostly in the beginning of community growth, when urea and the availability of other resources are highest. This phenotype is particularly interesting given *Microbacterium* is not the primary urea degrader or capable of bicarbonate production via carbonic anhydrase so should be expected to play a relatively small role in urea degradation. Though we did not see evidence of conversion of asparagine into ammonia for nitrogen, glutamine is the major, well-documented source of nitrogen for *Microbacterium* for tolerating pH induced stress. Both glutamine and nitrogen molecules were depleted after growth, indicating that the ammonia created by MICP may not be available to *Microbacterium. Microbacterium* has been shown to remodel TCA cycle metabolism in hypoxic environments, resulting in increased succinate and membrane potential, though we only find evidence of increased succinate in *R. qingshengii* profiles. Given the downregulation seen in Ile-Leu, Val-Thr, and other branched chain amino acids, it is likely that these mechanisms for reducing stress are taking place. *R. qingshengii* uses a different set of reactions relating to glutamate, and we find evidence of significant DE in oxoglutarate metabolism in the multi-evidence reaction network, primarily decreased in *R. qingshengii* and *B. toyonensis* and increased in *Microbacterium*. Thus, we find clear evidence glutamate is a hub compound for urea degradation in CSC-A, albeit through a complex, multi-pathway metabolic network. Further work is needed to determine the precise metabolic significance of Succinate and L-Phenylalanine, two other hub molecules with broad microbial biological activity.

This study, while comprehensive in an assessment of community level changes during urea degradation, did not fully perturb the community structure. This means we have not observed the effect of removing *B. toyonensis* or *Microbacterium* on community metabolic function. With the removal of *R. qingshengii, B. toyonensis* produced the largest change in transcription, suggesting it could overlap metabolically with much of the niche space that *R. qingshengii* currently utilizes. More phenotypic and genomic analysis is required to characterize the potentially novel *Microbacterium.* Depletion of amino acids, as was seen after growth in urea, has been suggested as a community strategy to modulate nitrogen metabolism to prevent competitors from accessing easy nitrogen sources. This could be negatively impacting community MICP and growth in urea. Further work engineering the bacterial nitrogen regulatory system to reduce the ability to switch between nitrogen sources is needed. Finally, a more thorough exploration of metabolic potential could be conducted by more phenotypic testing, such as carbon source growth assays or computational modeling techniques such as genome scale modeling, to gain a better

understanding of how community dynamics result in growth and production of metabolites.

Our study finds that CSC-A contains members with a diverse suite of metabolic potential, and phenotypic evidence of niche specialization in stress response and metabolism, as well as generalization in key metabolic functions such as denitrification. MICP holds promise as a biologically based method of carbon sequestration and industrial tool, and we demonstrate that a soil-based microbial consortia adapts to *in vitro* bioproduction by forming a multi-member nitrogen metabolism reaction network. There is still much unknown about the mechanistic driving forces behind community-enabled MICP, but this study highlights the strength gained from integrating multiple 'omic analysis. Future work, engineering new niche restrictions or enhancing calcium carbonate precipitation, can now be attempted to increase the efficiency and productivity of this novel biosystem.

4.0 References

Abdelsamad, Rim, Zulfa Al Disi, Mohammed Abu-Dieyeh, Mohammad A Al-Ghouti, and Nabil Zouari. 2022. "Evidencing the role of carbonic anhydrase in the formation of carbonate minerals by bacterial strains isolated from extreme environments in Qatar." *Heliyon* 8 (10).

Adingo, Samuel, Jie-Ru Yu, Liu Xuelu, Xiaodan Li, Sun Jing, and Zhang Xiaong. 2021. "Variation of soil microbial carbon use efficiency (CUE) and its Influence mechanism in the context of global environmental change: A review." *PeerJ* 9: e12131.

Chittoori, Bhaskar CS, Malcolm Burbank, and Md Touhidul Islam. 2018. "Evaluating the effectiveness of soil-native bacteria in precipitating calcite to stabilize expansive soils." In *IFCEE 2018*, 59-68.

Dhami, Navdeep K, M Sudhakara Reddy, and Abhijit Mukherjee. 2013. "Biomineralization of calcium carbonates and their engineered applications: a review." *Frontiers in microbiology* 4: 314.

feng Su, Jun, Lei Xue, Ting lin Huang, Li Wei, Chun yu Gao, and Qiong Wen. 2019. "Performance and microbial community of simultaneous removal of NO3−-N, Cd2+ and Ca2+ in MBBR." *Journal of environmental management* 250: 109548.

Fierer, Noah, and Corinne M Walsh. 2023. "Can we manipulate the soil microbiome to promote carbon sequestration in croplands?" *PLoS Biology* 21 (7): e3002207.

Fu, Tianzheng, Alexandra Clarà Saracho, and Stuart Kenneth Haigh. 2023. "Microbially induced carbonate precipitation (MICP) for soil strengthening: A comprehensive review." *Biogeotechnics* 1 (1): 100002.

Fujita, Yoshiko, F Grant Ferris, R Daniel Lawson, Frederick S Colwell, and Robert W Smith. 2000. "Subscribed content calcium carbonate precipitation by ureolytic subsurface bacteria." *Geomicrobiology Journal* 17 (4): 305-318.

Giri, Anand, and Deepak Pant. 2019. "CO2 management using carbonic anhydrase producing microbes from western Indian Himalaya." *Bioresource Technology Reports* 8: 100320.

Gorter, Florien A, Michael Manhart, and Martin Ackermann. 2020. "Understanding the evolution of interspecies interactions in microbial communities." *Philosophical Transactions of the Royal Society B* 375 (1798): 20190256.

Herrera Paredes, Sur, Tianxiang Gao, Theresa F Law, Omri M Finkel, Tatiana Mucyn, Paulo José Pereira Lima Teixeira, Isaí Salas González, Meghan E Feltcher, Matthew J Powers, and Elizabeth A Shank. 2018. "Design of synthetic bacterial communities for predictable plant phenotypes." *PLoS biology* 16 (2): e2003962.

Heyse, Jasmine, Benjamin Buysschaert, Ruben Props, Peter Rubbens, Andre G Skirtach, Willem Waegeman, and Nico Boon. 2019. "Coculturing bacteria leads to reduced phenotypic heterogeneities." *Applied and environmental microbiology* 85 (8): e02814-18.

Jean-Pierre, Fabrice, Thomas H Hampton, Daniel Schultz, Deborah A Hogan, Marie-Christine Groleau, Eric Déziel, and George A O'Toole. 2023. "Community composition shapes microbial-specific phenotypes in a cystic fibrosis polymicrobial model system." *Elife* 12: e81604.

Korenblum, Elisa, Yonghui Dong, Jedrzej Szymanski, Sayantan Panda, Adam Jozwiak, Hassan Massalha, Sagit Meir, Ilana Rogachev, and Asaph Aharoni. 2020. "Rhizosphere microbiome mediates systemic root metabolite exudation by root-to-root signaling." *Proceedings of the National Academy of Sciences* 117 (7): 3874-3883.

Lal, Rattan. 2004. "Soil carbon sequestration impacts on global climate change and food security." *science* 304 (5677): 1623-1627.

Lamb, Austin, Brock Weers, Brian McKinley, William Rooney, Cristine Morgan, Amy Marshall-Colon, and John Mullet. 2022. "Bioenergy sorghum's deep roots: A key to sustainable biomass production on annual cropland." *GCB Bioenergy* 14 (2): 132-156.

Letek, Michal, Patricia Gonzalez, Iain MacArthur, Héctor Rodríguez, Tom C Freeman, Ana Valero-Rello, Monica Blanco, Tom Buckley, Inna Cherevach, and Ruth Fahey. 2010. "The genome of a pathogenic Rhodococcus: cooptive virulence underpinned by key gene acquisitions." *PLoS genetics* 6 (9): e1001145.

Liu, Nana, Huifeng Hu, Wenhong Ma, Ye Deng, Qinggang Wang, Ao Luo, Jiahui Meng, Xiaojuan Feng, and Zhiheng Wang. 2021. "Relative importance of deterministic and stochastic processes on soil microbial community assembly in temperate grasslands." *Microorganisms* 9 (9): 1929.

Liu, Peng, Yu Zhang, Qiang Tang, and Shenjie Shi. 2021. "Bioremediation of metal-contaminated soils by microbially-induced carbonate precipitation and its effects on ecotoxicity and long-term stability." *Biochemical Engineering Journal* 166: 107856.

Liu, Xiaoxia, Gernot Zarfel, Renata van der Weijden, Willibald Loiskandl, Brigitte Bitschnau, Inez JT Dinkla, Elmar C Fuchs, and Astrid H Paulitsch-Fuchs. 2021. "Density-dependent microbial calcium carbonate precipitation by drinking water bacteria via amino acid metabolism and biosorption." *Water Research* 202: 117444.

Lozano, Gabriel L, Juan I Bravo, Manuel F Garavito Diago, Hyun Bong Park, Amanda Hurley, S Brook Peterson, Eric V Stabb, Jason M Crawford, Nichole A Broderick, and Jo Handelsman. 2019. "Introducing THOR, a model microbiome for genetic dissection of community behavior." *MBio* 10 (2): 10.1128/mbio. 02846-18.

Mason, ARG, MJ Salomon, AJ Lowe, and TR Cavagnaro. 2023. "Microbial solutions to soil carbon sequestration." *Journal of Cleaner Production*: 137993.

Mazzei, Luca, Francesco Musiani, and Stefano Ciurli. 2020. "The structure-based reaction mechanism of urease, a nickel dependent enzyme: tale of a long debate." *JBIC Journal of Biological Inorganic Chemistry* 25 (6): 829-845.

McClure, R., D. Naylor, Y. Farris, M. Davison, S. J. Fansler, K. S. Hofmockel, and J. K. Jansson. 2020. "Development and Analysis of a Stable, Reduced Complexity Model Soil Microbiome." *Front Microbiol* 11: 1987. https://doi.org/10.3389/fmicb.2020.01987. https://www.ncbi.nlm.nih.gov/pubmed/32983014.

McClure, Ryan, Yuliya Farris, Robert Danczak, William Nelson, Hyun-Seob Song, Aimee Kessell, Joon-Yong Lee, Sneha Couvillion, Christopher Henry, and Janet K Jansson. 2022. "Interaction networks are driven by community-responsive phenotypes in a chitin-degrading consortium of soil microbes." *Msystems* 7 (5): e00372-22.

McClure, Ryan, Marci Garcia, Sneha Couvillion, Yuliya Farris, and Kirsten S Hofmockel. 2023. "Removal of primary nutrient degraders reduces growth of soil microbial communities with genomic redundancy." *Frontiers in Microbiology* 13: 1046661.

Morris, Brandon EL, Ruth Henneberger, Harald Huber, and Christine Moissl-Eichinger. 2013. "Microbial syntrophy: interaction for the common good." *FEMS microbiology reviews* 37 (3): 384-406.

Naeimi, Maryam, Jian Chu, Mohammad Khosroshahi, and Leila Kashi Zenouzi. 2023. "Soil stabilization for dunes fixation using microbially induced calcium carbonate precipitation." *Geoderma* 429: 116183.

Naylor, Dan, Sarah Fansler, Colin Brislawn, William C Nelson, Kirsten S Hofmockel, Janet K Jansson, and Ryan McClure. 2020. "Deconstructing the soil microbiome into reduced-complexity functional modules." *MBio* 11 (4): e01349-20.

Occhipinti, Rossana, and Walter F Boron. 2019. "Role of carbonic anhydrases and inhibitors in acid–base physiology: insights from mathematical modeling." *International journal of molecular sciences* 20 (15): 3841.

Okyay, Tugba O, Hang N Nguyen, Sarah L Castro, and Debora F Rodrigues. 2016. "CO2 sequestration by ureolytic microbial consortia through microbially-induced calcite precipitation." *Science of the Total Environment* 572: 671-680.

Park, Inmyoung, Young-Su Seo, and Mohamed Mannaa. 2023. "Recruitment of the rhizo-microbiome army: assembly determinants and engineering of the rhizosphere microbiome as a key to unlocking plant potential." *Frontiers in Microbiology* 14: 1163832.

Phillips, Adrienne J, Robin Gerlach, Ellen Lauchnor, Andrew C Mitchell, Alfred B Cunningham, and Lee Spangler. 2013. "Engineered applications of ureolytic biomineralization: a review." *Biofouling* 29 (6): 715-733.

Saraiva, Joao Pedro, Anja Worrich, Canan Karakoç, Rene Kallies, Antonis Chatzinotas, Florian Centler, and Ulisses Nunes da Rocha. 2021. "Mining synergistic microbial interactions: a roadmap on how to integrate multi-omics data." *Microorganisms* 9 (4): 840.

Shayanthan, Ambihai, Patricia Ann C Ordoñez, and Ivan John Oresnik. 2022. "The Role of Synthetic Microbial Communities (SynCom) in Sustainable Agriculture." *Frontiers in Agronomy*: 58.

Sparks, Donald L, Balwant Singh, and Matthew G Siebecker. 2022. *Environmental soil chemistry*. Elsevier.

Stocks-Fischer, Shannon, Johnna K Galinat, and Sookie S Bang. 1999. "Microbiological precipitation of CaCO3." *Soil Biology and Biochemistry* 31 (11): 1563-1571.

Supuran, Claudiu T, and Clemente Capasso. 2017. "An overview of the bacterial carbonic anhydrases." *Metabolites* 7 (4): 56.

Tripathi, Binu M, James C Stegen, Mincheol Kim, Ke Dong, Jonathan M Adams, and Yoo Kyung Lee. 2018. "Soil pH mediates the balance between stochastic and deterministic assembly of bacteria." *The ISME journal* 12 (4): 1072-1083.

Wang, Sheng, Longyang Fang, Malcom Frimpong Dapaah, Qijian Niu, and Liang Cheng. 2023. "Bio-Remediation of Heavy Metal-Contaminated Soil by Microbial-Induced Carbonate Precipitation (MICP)—A Critical Review." *Sustainability* 15 (9): 7622.

Wang, Yuze, Charalampos Konstantinou, Sikai Tang, and Hongyu Chen. 2023. "Applications of microbial-induced carbonate precipitation: A state-of-the-art review." *Biogeotechnics*: 100008.

Xu, Jing-Liang, Jian He, Zhi-Chun Wang, Kun Wang, Wen-Jun Li, Shu-Kun Tang, and Shun-Peng Li. 2007. "Rhodococcus qingshengii sp. nov., a carbendazim-degrading bacterium." *International journal of systematic and evolutionary microbiology* 57 (12): 2754-2757.

Yoshida, Naoto, Eiji Higashimura, and Yuichi Saeki. 2010. "Catalytic biomineralization of fluorescent calcite by the thermophilic bacterium Geobacillus thermoglucosidasius." *Applied and environmental microbiology* 76 (21): 7322-7327.

Zamanian, Kazem, Jianbin Zhou, and Yakov Kuzyakov. 2021. "Soil carbonates: The unaccounted, irrecoverable carbon source." *Geoderma* 384: 114817.

Zambare, Neerja M, Nada Y Naser, Robin Gerlach, and Connie B Chang. 2020. "Mineralogy of microbially induced calcium carbonate precipitates formed using single cell drop-based microfluidics." *Scientific reports* 10 (1): 17535.

Zegeye, E. K., C. J. Brislawn, Y. Farris, S. J. Fansler, K. S. Hofmockel, J. K. Jansson, A. T. Wright, E. B. Graham, D. Naylor, R. S. McClure, and H. C. Bernstein. 2019. "Selection, Succession, and Stabilization of Soil Microbial Consortia." *mSystems* 4 (4). https://doi.org/10.1128/mSystems.00055-19. https://www.ncbi.nlm.nih.gov/pubmed/31098394.

Zhou, Jizhong, and Daliang Ning. 2017. "Stochastic community assembly: does it matter in microbial ecology?" *Microbiology and Molecular Biology Reviews* 81 (4): 10.1128/mmbr.00002-17.

Zhu, Tingting, and Maria Dittrich. 2016. "Carbonate precipitation through microbial activities in natural environment, and their potential in biotechnology: a review." *Frontiers in bioengineering and biotechnology* 4: 4.

Zhu, Xinyu, Stefano Campanaro, Laura Treu, Rekha Seshadri, Natalia Ivanova, Panagiotis G Kougias, Nikos Kyrpides, and Irini Angelidaki. 2020. "Metabolic dependencies govern microbial syntrophies during methanogenesis in an anaerobic digestion ecosystem." *Microbiome* 8 (1): 1-14.

Zhu, Xuejiao, Weila Li, Lu Zhan, Minsheng Huang, Qiuzhuo Zhang, and Varenyam Achal. 2016. "The large-scale process of microbial carbonate precipitation for nickel remediation from an industrial soil." *Environmental Pollution* 219: 149-155.

Zuñiga, Cristal, Chien-Ting Li, Geng Yu, Mahmoud M Al-Bassam, Tingting Li, Liqun Jiang, Livia S Zaramela, Michael Guarnieri, Michael J Betenbaugh, and Karsten Zengler. 2019. "Environmental stimuli drive a transition from cooperation to competition in synthetic phototrophic communities." *Nature microbiology* 4 (12): 2184-2191.

Pacific Northwest National Laboratory

902 Battelle Boulevard
P.O. Box 999
Richland, WA 99354

1-888-375-PNNL (7665)

www.pnnl.gov